ACS OMEGA

http://pubs.acs.org/journal/acsodf

Article

Novel TRPV1 Modulators with Reduced Pungency Induce Analgesic Effects in Mice

Anny Treat,[⊥] Vianie Henri,[⊥] Junke Liu,[⊥] Joyce Shen, Mauricio Gil-Silva, Alejandro Morales, Avaneesh Rade, Kevin Joseph Tidgewell, Benedict Kolber,* and Young Shen*

Cite This: *ACS Omega* 2022, 7, 2929−2946

Read Online

ACCESS | Metrics & More | Article Recommendations | Supporting Information

ABSTRACT: Capsaicin, the compound in hot chili peppers responsible for their pungency and an agonist of the transient receptor potential cation channel, subfamily V, member 1 (TRPV1), has long been known to promote the desensitization of nociceptors at high concentrations. This has led to the utilization and implementation of topical capsaicin cream as an analgesic to treat acute and chronic pain. Critically, the application of capsaicin cream is limited due to capsaicin's high pungency, which is experienced prior to analgesia. To combat this issue, novel capsaicin analogues were developed to provide analgesia with reduced pungency. Analogues reported in this paper add to and show some differences from previous structure−activity relationship (SAR) studies of capsaicin-like molecules against TRPV1, including the necessity of phenol in the aromatic "A-region", the secondary amide in the "B-region", and modifications in the hydrophobic "C-region". This provided a new framework for *de novo* small-molecule design using capsaicin as the starting point. In this study, we describe the synthesis of capsaicin analogues, their *in vitro* activity in Ca^{2+} assays, and initial *in vivo* pungency and feasibility studies of capsaicin analogues YB-11 and YB-16 as analgesics. Our results demonstrate that male and female mice treated with YB capsaicin analogues showed diminished pain-associated behavior in the spontaneous formalin assay as well as reduced thermal sensitivity in the hotplate assay.

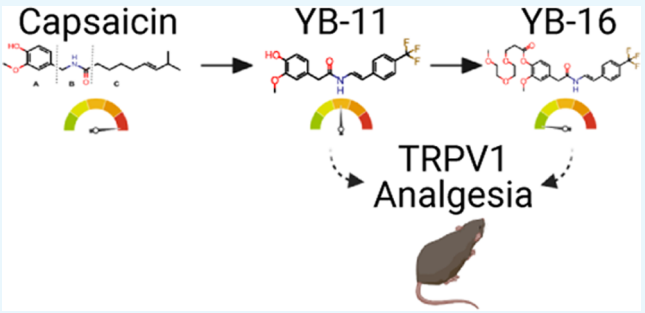

INTRODUCTION

Chronic pain, defined as persistent pain that lasts for a minimum of 3 months, affects more than 100 million adults in the United States.[1] Those who suffer from chronic pain are also likely to develop feelings of depression and anxiety that greatly affect their quality of life.[2] Opioids remain the most prescribed class of medications used to help manage the pain experienced by chronic pain patients.[3] Unfortunately, the high abuse and addiction potential of opioids has led to the current public health crisis known as the opioid epidemic. One current alternative to opioid prescriptions is topical analgesics, such as creams and dermal patches, that use capsaicin as the main therapeutic ingredient.

Capsaicin is the active compound in hot chili peppers responsible for their pungent taste and it is one of the most studied natural products with analgesic activity.[4−8] Capsaicin is an agonist of the transient receptor potential cation channel, subfamily V, member 1 (TRPV1), also known as the vanilloid receptor type 1 (VR1).[6,8] TRPV1 receptors are nonselective cation channels expressed primarily in small diameter nociceptive afferents and are activated by high noxious temperatures, acidic pH, and some endogenous lipids.[6,9−11] The immediate effects of capsaicin stimulation of TRPV1-positive nociceptors include an increase in intracellular calcium, membrane depolarization, and the increased firing rate of peripheral nociceptors. After this immediate phase, capsaicin can render nociceptors insensitive to further noxious stimuli, a process referred to as desensitization, or defunctionalization, of the nociceptive afferents. Sustained high intracellular Ca^{2+} levels likely cause multiple events that lead to nociceptor defunctionalization, including the inhibition of ion channels, inhibition of protein synthesis, microtubule disassembly, mitochondrial dysfunction, and loss of plasma membrane stability.[12−15] These changes in neuronal cell physiology ultimately lead to the retraction of nociceptive nerve terminals.[16,17] This leads to analgesia as a temporally delayed effect of capsaicin treatment.

While capsaicin can alleviate chronic pain, the use of capsaicin is presented with many negatives. When used topically, capsaicin can cause acute dermal irritation erythema and a burning sensation. This requires the use of low doses of

Received: October 20, 2021
Accepted: December 31, 2021
Published: January 10, 2022

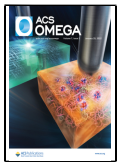

https://doi.org/10.1021/acsomega.1c05727
ACS Omega 2022, 7, 2929−2946

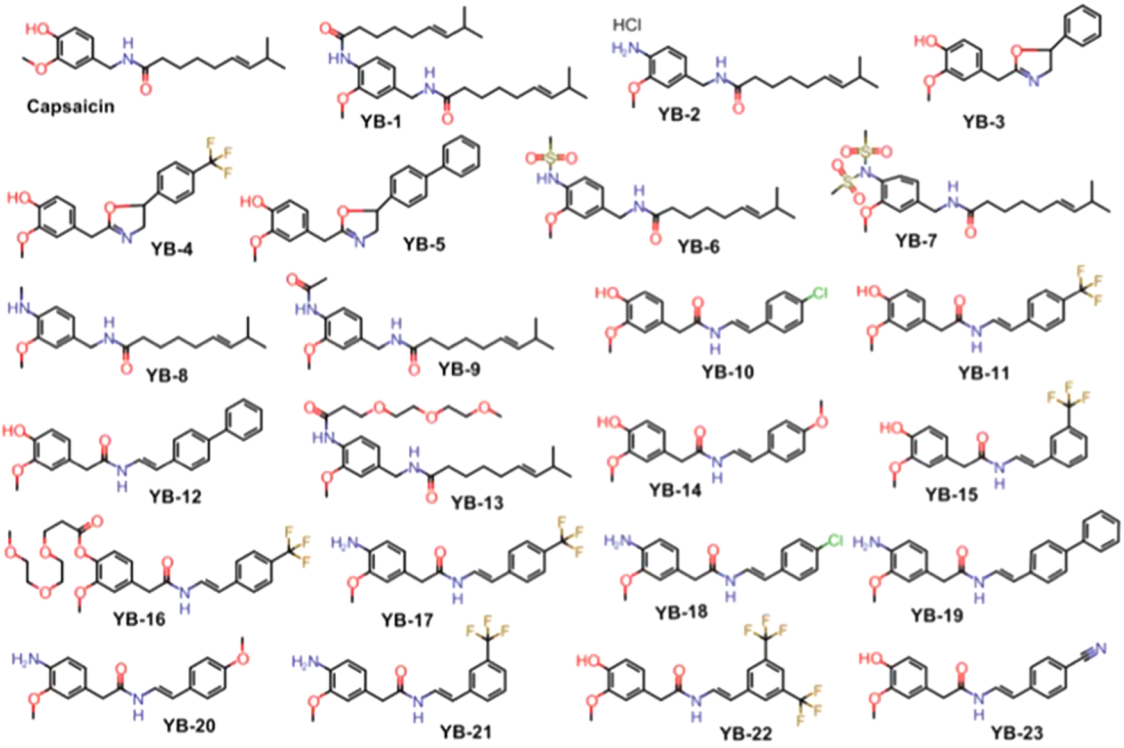

Figure 1. Structures of capsaicin and synthetic analogues.

capsaicin to prevent deleterious side effects.[10] Over-the-counter (OTC) capsaicin cream is formulated in doses of 0.0025 and 0.075% that require application 3−4 times daily. Clinical studies find that these doses yield moderate-to-poor results for the relief of chronic neuropathic pain.[10] However, higher doses of capsaicin can lead to severe side effects; in a study that utilized 5, 7.5, and 10% topical capsaicin, patients required epidural anesthesia to be able to tolerate the intense immediate effects of these high doses.[18] Currently, the capsaicin 8% patch (C8P) is a one-application topical treatment with a formula concentration 100 times higher than that of OTC capsaicin treatments. As expected, the use of C8P again results in transient side effects that include redness of the skin and pain.[10]

Another confounding factor in developing capsaicin-based therapeutics is its low aqueous solubility.[19] Additionally, although early studies in animals demonstrated that the systemic administration of capsaicin alleviated pain, high doses of capsaicin produced toxic effects including the induction of convulsions, loss of mean arterial pressure, and death.[20] Thus, capsaicin-based treatments have been limited to topical administration.

The robust pungency of capsaicin is suspected to be the cause of many of the deleterious side effects associated with high doses of capsaicin.[21] However, several studies have demonstrated that the pungency of capsaicin analogues can be separated from their potency for TRPV1 receptors or rather pungency is not required for TRPV1 activation.[22,23] TRPV1 has a complex polymodal activation profile, and selective TRPV1 modulators may interfere with only a subset of the activation modalities, resulting in the reduction of pungency and side effects.[24,25] For example, capsiate, a nonpungent capsaicin-like compound, was able to activate TRPV1 receptors without inducing pungency-associated responses when applied to the skin surface, eyes, or oral cavities of mice.[26] Furthermore, the intraplantar injection of olvanil, a TRPV1 agonist devoid of pungency, produced a robust analgesic effect in rats without inducing hyperalgesia immediately following application.[22] This line of evidence has led to the hypothesis that nonpungent capsaicin analogues may be used in clinical settings to produce analgesia with fewer side effects than capsaicin-based treatments.

To combat the issues of low aqueous solubility and high pungency, capsaicin was chemically modified to yield analogues referred to here as "YB" capsaicinoids (Figure 1), of which YB-11 and YB-16 proved to be the most promising. Our results suggest that these novel capsaicin analogues can be used as an alternative to capsaicin in highly efficacious doses to achieve analgesia with reduced irritation, erythema, and burning pain associated with capsaicin treatments.

RESULTS

***In Vitro* Screening and Structure−Activity Relationship (SAR) Findings.** Capsaicin-like TRPV1 agonists with potent *in vitro* activity (EC_{50} < 1 μM in the Ca^{2+} flux assay) are proven to show significant analgesic properties *in vivo*.[27] We sought to improve on existing compounds by reducing pungency while maintaining analgesic potential. Using capsaicin (Figure 2) as the parent molecule, we built a series

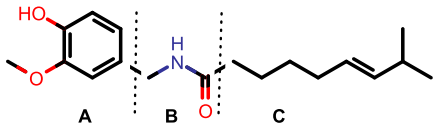

Figure 2. Structure of capsaicin. To probe the SAR of capsaicin, three series of analogues were synthesized that modified the aromatic ring (A), the amide region (B), and the hydrophobic side chain (C) of the compound.

https://doi.org/10.1021/acsomega.1c05727
ACS Omega 2022, 7, 2929−2946

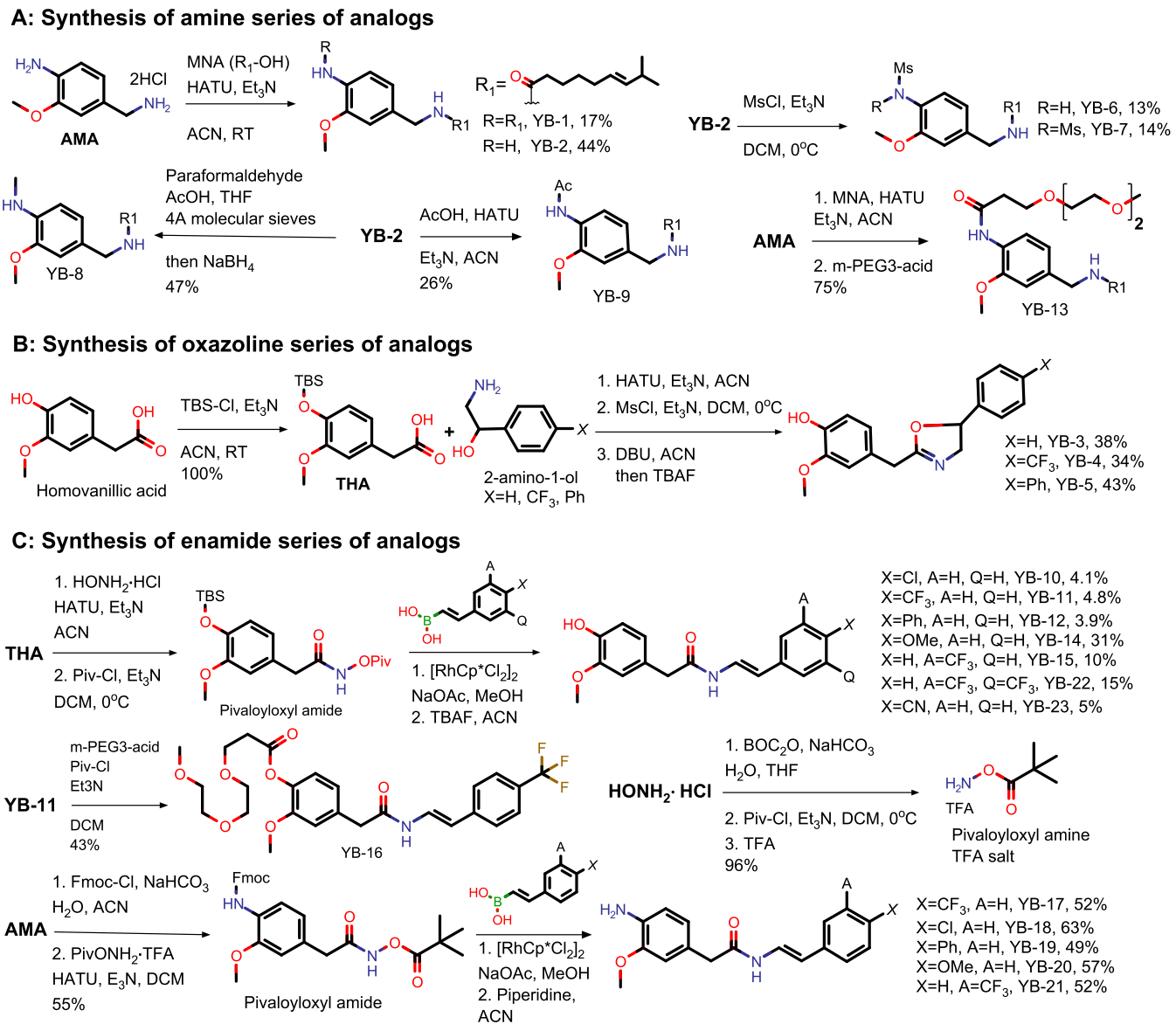

Figure 3. Synthesis of three series of YB analogues. (A) The amide series; (B) the oxazoline series; and (C) the enamide series.

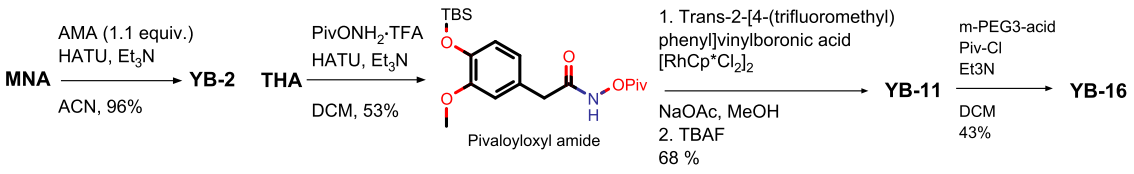

Figure 4. Optimization of YB-2, YB-11, and YB-16 syntheses.

of novel analogues ("YB" compounds; Figures 1, 3, and 4). We first determined whether YB analogues were potent TRPV1 agonists. To this end, we transiently transfected TRPV1 into HEK-293 cells (Figure 5) and determined the EC_{50} of all YB analogues using a Ca^{2+} flux assay in 96-well plates.[28] Eighteen analogues were active with EC_{50}s <10 μM, and four analogues (YB-2, 10, 11, and 15) were more potent than capsaicin (Table 1).

The results of these Ca^{2+} flux assays significantly expand the understanding of the SAR of capsaicin in three ways from that of previous reports, which were restricted by capsaicin's limited natural availability and low structural variability. First, the modification of the phenol functional group in the aromatic region (the "A-region") by previous groups resulted in the loss of activity,[27] leading to the conclusion that this phenol group was critical for the activity of capsaicin. However, we found promising activities of analogues YB-2, 8, 9, 13, 17, 18, 20, and 21 (Table 1), which demonstrate that the phenol group can be replaced with alternative polar groups such as amine or amide groups. Second, the NH group in the amide bond (the "B-region") was considered necessary for activity.[29] However, we found that in the absence of an NH group in the B-region, our oxazoline analogues YB-4 (EC50 = 0.68 ± 0.12 μM) and YB-5 (EC_{50} = 2.0 ± 0.29 μM) still showed activity for TRPV1. This

https://doi.org/10.1021/acsomega.1c05727
ACS Omega 2022, 7, 2929−2946

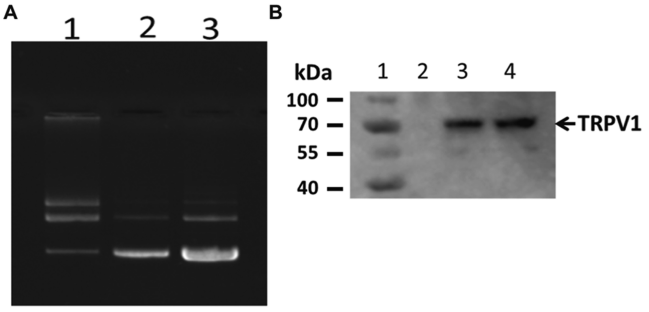

Figure 5. Purification and expression of TRPV1. (A) Large-scale purification of TRPV1/pcDNA3.1+/C-(K)DYK plasmid DNA. Lane 1: 300 ng (parental plasmid DNA); lane 2: 200 ng newly purified plasmid; and lane 3: 400 ng newly purified plasmid. (B) TRPV1 protein expression in HEK-293 cells detected by Western blot. Lane 1: protein ladder; lane 2: HEK-293 cell alone; lane 3: 18 h post-transfection; and lane 4: 23 h post-transfection.

Table 1. *In Vitro* Human TRPV1 Agonistic Activities[a]

compound	EC_{50} (μM)
capsaicin	0.11 ± 0.021
YB-1	27 ± 3.8
YB-2	0.082 ± 0.015
YB-3	>10
YB-4	0.68 ± 0.12
YB-5	2.0 ± 0.29
YB-6	>10
YB-7	>10
YB-8	1.9 ± 0.23
YB-9	0.96 ± 0.12
YB-10	0.047 ± 0.0075
YB-11	0.012 ± 0.0033
YB-12	0.60 ± 0.069
YB-13	3.1 ± 0.41
YB-14	0.33 ± 0.041
YB-15	0.048 ± 0.0057
YB-16	0.93 ± 0.082
YB-17	1.1 ± 0.29
YB-18	1.0 ± 0.20
YB-19	45 ± 3.3
YB-20	4.9 ± 0.73
YB-21	0.34 ± 0.065
YB-22	0.21 ± 0.052
YB-23	0.30 ± 0.074

[a]EC_{50} data represent mean ± standard error of the mean (SEM) from three independent experiments. Images in Figure 1 show chemical structures for all referenced analogues in Table 1.

demonstrates that N-methylation of the amide group (capsaicin analogue 3d in ref 35; EC_{50} > 100 μM in the Ca^{2+} influx assay) likely affects the conformation of the molecule, rather than disrupting the amide NH group from acting as a hydrogen-bonding donor to the TRPV1 receptor. This is consistent with the low-energy conformations calculated by MOE 2020.0901 using the LowModeMD method (Chemical Computing Group). Low-energy conformation of capsaicin is similar to that of YB-4 and is quite different from that of N-Me capsaicin (Figure 6). This is also supported by the lack of direct interaction between the capsaicin amide NH group and TRPV1 receptor based on the analysis of the cryoEM structure of capsaicin bound to TRPV1 (Figure 7).

Third, the overall size and hydrophobicity were considered more important than the detailed structural variations in the hydrophobic side-chain "C-region".[30] Although the cryoEM structures indicate that lipophilicity is a key driver of activity in this region of the molecule and the binding pocket has ample space, detailed structural variations can still make a significant impact on the activity. The structures of oxazoline analogues YB-3, 4, and 5 are similar, their activities are quite different, and YB-4 with a trifluoromethyl substitution on the side chain is most potent with an EC_{50} of 0.68 μM. Similarly, the structures of enamide analogues YB-10, 11, 12, 14, 15, 22, and 23 are similar, their activities are quite different, and analogues YB-10, YB-11, and YB-15, with a trifluoromethyl substitution or a chloro substitution on the side chain, are most potent with EC_{50}s of 0.012−0.048 μM (Table 1). Similarly, structures of enamide amine analogues YB-17−21 are similar, their activities were quite different, and analogues YB-17, 18, and 21 with a trifluoromethyl substitution or a chloro substitution on the side chain were most potent with EC_{50}s of 0.34−1.1 μM. This suggests the importance of certain structural features with appropriate size and lipophilicity on the side chain. Excessive size and lipophilicity can reduce the activity (CF_3-substituted analogue YB-11: EC_{50} 0.012 μM vs di-CF3-substituted analogue YB-22: EC_{50} 0.21 μM vs Ph-substituted analogue YB-12: EC_{50} 0.60 μM) and possibly lead to poor solubility and other undesired drug properties, *e.g.*, resiniferatoxin (RTX), a potent TRPV1 agonist with a large lipophilic side chain in region C, is insoluble in water and toxic.[25]

In addition, our analogues enabled further insights into drug structural motifs. Enamides are thought to represent key structural motifs in various bioactive natural products.[31] We found that the introduction of a rigid *trans*-enamide motif in enamide phenol analogues provided favorable conformation for TRPV1 binding and increased the potency. Enamide phenol analogue YB-11 showed the highest potency with an EC_{50} of 0.012 μM. Introduction of the *trans*-enamide motif in aniline analogues decreased the potency (YB-17 EC_{50} of 1.1 μM vs YB-11 EC_{50} of 0.012 μM), possibly due to the added desolvation energy required for the aniline. Finally, we found that introducing a polar poly(ethylene glycol) (PEG) substitution on the aniline and phenol groups resulted in decreased potency (YB-13 EC_{50} of 3.1 μM vs YB-2 EC_{50} of 0.082 μM; YB-16 EC_{50} of 0.93 μM vs YB-11 EC_{50} of 0.012 μM), with a greater negative impact on the phenol than on the aniline.

After this initial characterization of the YB family, we chose to pursue a more detailed analysis of a select group of YB compounds including YB-2, the most potent analogue from the amine series, and the most potent analogue YB-11 with its prodrug YB-16 from the enamide series (Figure 8 shows YB-16 and YB-11).

Structural Modifications Reduced Pungency. As noted in the Introduction section, capsaicin is confined to topical use at low concentration due to its pungency and solubility limitations. To evaluate this issue, three analogues (YB-2, 11, and 16) were selected for rodent eye wiping pungency testing. Suggesting the potential to overcome the pungency limitation of the parent capsaicin, we show that all of these novel compounds caused lower relative pain-producing potency (RPP) than capsaicin, with YB-16 showing >7-fold reduction in pungency (Table 2 and Figure 9). These results indicated that the undesired pungency in capsaicin can be reduced by structural modifications similar to what was previously known

https://doi.org/10.1021/acsomega.1c05727
ACS Omega 2022, 7, 2929−2946

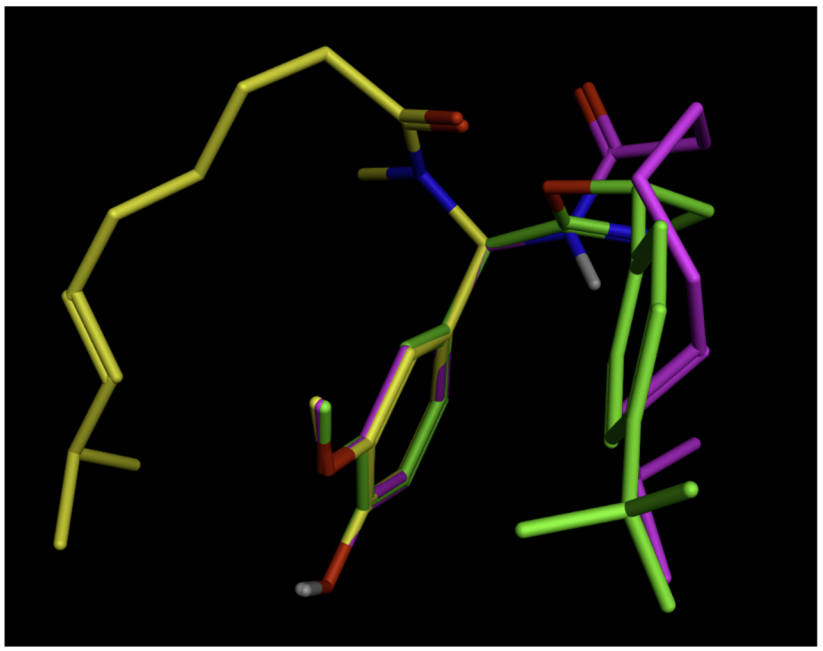

Figure 6. Low-energy conformations: capsaicin (magenta), YB-4 (green), and N-Me capsaicin (yellow). MOE 2020.0901: LowModeMD method (Chemical Computing Group).

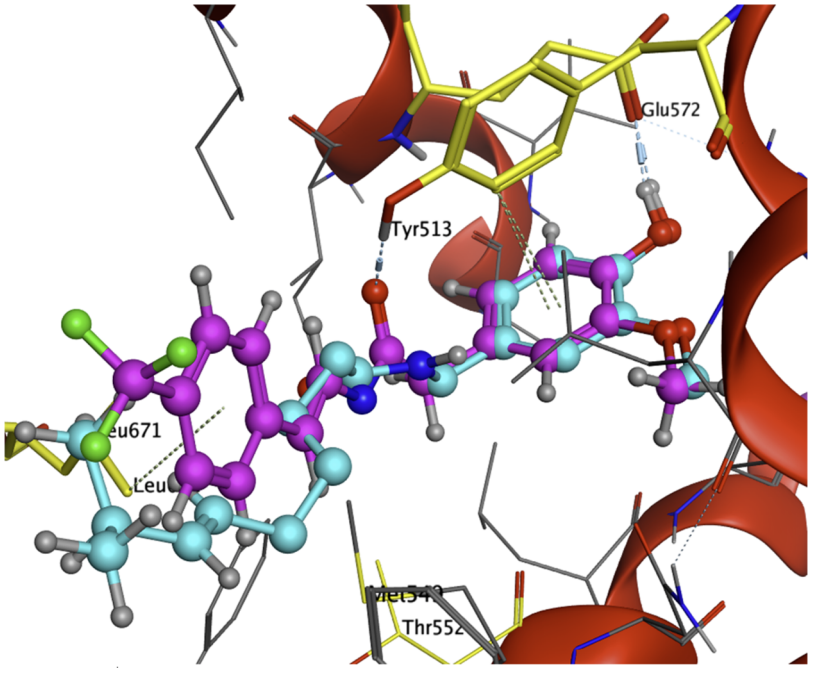

Figure 7. Computational analysis of YB-11 and capsaicin in TRPV1 binding pocket (YB-11 in magenta and capsaicin in cyan). Computational analysis was carried out using computer modeling software MOE 2020.0901 (Chemical Computing Group). Structural data of squirrel TRPV1 in complex with capsaicin with PDB ID 7LR0 (RCSB Protein Data Bank deposition authors: Neuberger, A., Nadezhdin, K. D., Sobolevsky, A. I.) were used to build the model.

from capsiate and other related compounds. Additional analogues will be tested to further investigate the SAR of pungency effect in the future.

Select YB Analogues Desensitize TRPV1 *In Vitro*. To further evaluate the impact of YB analogues on the classic TRPV1 function, we tested YB-11 and 16 in primary mouse dorsal root ganglion (DRG) neurons using Ca^{2+} imaging. DRG neurons respond to capsaicin with an extracellular Ca^{2+} influx that desensitizes with multiple bath applications of the capsaicin.[32,33] Corroborating these data, we found that 0.5 μM capsaicin reduced the subsequent application of 0.5 μM capsaicin with 68−71 (96%) TRPV1-sensitive neurons showing desensitization (Figure 10A−C). This included a statistically significant reduction in the max signal of the second application (paired *t*-test $P < 0.0001$; Figure 10B) and area under the curve of the second application (paired *t*-test $P < 0.0001$; Figure 10C). Next, we repeated this experiment but used YB-11 and 16 as the first treatment compounds followed

https://doi.org/10.1021/acsomega.1c05727
ACS Omega 2022, 7, 2929−2946

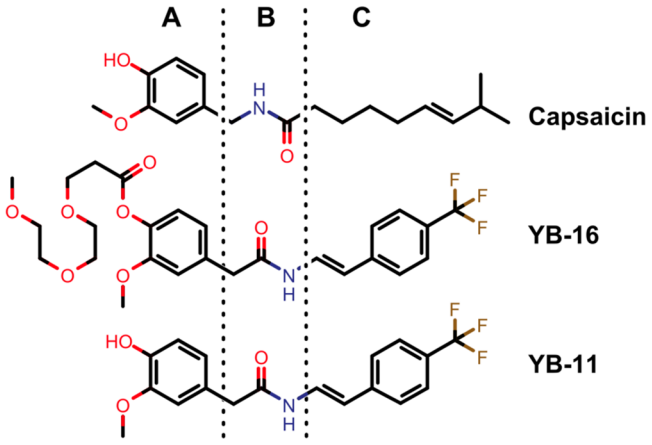

Figure 8. Structures of capsaicin, YB-16, and YB-11. (A) Aromatic region; (B) amide linker region; and (C) lipophilic side-chain region.

Table 2. Pungency Comparison from Rodent Eye Wiping Assay[a]

compound	pungency (SHU)	MPP (mg/mL)	Pungency (RPP)
capsaicin	16 000 000	0.041	100
YB-2	n.t.	0.233	17.6
YB-11	n.t.	0.101	40.6
YB-16	n.t.	0.302	13.6

[a]SHUs, Scoville Heat Units; MPP, moderate pain-producing potency concentration; RPP, relative pain-producing potency with capsaicin set to 100; and n.t., not tested.

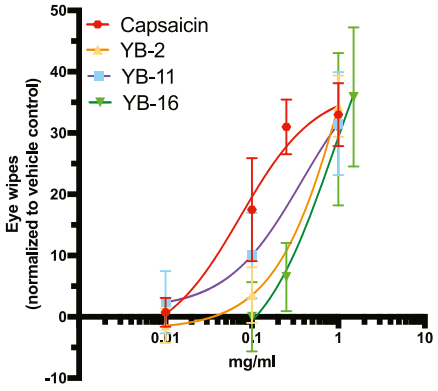

Figure 9. Dose−response curves for pungency analysis. Dose−response curves obtained based on the number of protective eye wipes after dilute concentrations were instilled into the eye of male and female mice (at least three concentrations per compound). $n = 8$ for capsaicin, YB-16. $n = 6$ for YB-2 and YB-11. Data are presented as normalized mean ± SEM. Eye wipes normalized to vehicle control ($n = 8$) response.

by capsaicin application in an identical time course to the double-capsaicin experiment. For YB-11, we found a strong Ca^{2+} signal after the YB-11 (0.5 μM) application along with a reduction in the subsequent capsaicin application with 34−51 (67%) TRPV1-sensitive neurons showing desensitization (Figure 10D−F). This included a statistically significant reduction in the max signal of the second application (paired t-test $P < 0.001$; Figure 10E) and area under the curve of the second application (paired t-test $P < 0.001$; Figure 10F). For YB-16, an initial experiment using 0.5 μM YB-16 found neither YB-16-induced activity nor capsaicin desensitization (mean peak fluorescence of 0.04 ± 0.09 for 0.5 μM YB-16 vs a mean peak fluorescence of 4.00 ± 0.38 for 0.5 μM capsaicin; data not shown). However, we found a strong Ca^{2+} signal after a higher 1.0 μM YB-16 application along with a reduction in the subsequent capsaicin (0.5 μM) application; 57 of 72 (79%) TRPV1-sensitive neurons showed desensitization (Figure 10G−I). This included a statistically significant reduction in the max signal of the second application (paired t-test $P < 0.0001$; Figure 10H) and area under the curve of the second application (paired t-test $P < 0.001$; Figure 10I). Overall, these data demonstrate that the tested YB compounds desensitize sensory neurons in a similar manner to the prototypical TRPV1 agonist capsaicin.

To evaluate the activation that occurs with the compound alone, we also analyzed the max activation and AUC for the first treatments in the above experiment. Although both YB-11 and YB-16 were able to activate DRG (compared to baseline), there is an apparent reduction in total activation compared to capsaicin alone. With one-way ANOVA, we found a statistically significant main effect of treatment ($P = 0.011$) on the max change in fluorescence (Figure 11A). Dunnett's post hoc analyses found significant decreases in max activation for both YB-11 ($P < 0.05$) and YB-16 ($P < 0.05$) compared to that for capsaicin. With one-way ANOVA, we found a statistically significant main effect of treatment ($P < 0.0001$) on the area under the curve (Figure 11B). Dunnett's post hoc analyses found significant decreases in the area under the curve for both YB-11 ($P < 0.0001$) and YB-16 ($P < 0.0001$) compared to that for capsaicin.

DMPK Evaluation for Selected YB Compounds. We worked with Charles River Laboratories in Worcester, MA, to conduct DMPK studies for selected YB compounds: YB-2 [*in vitro* DMPK and *in vivo* mouse PK (IV/PO)] and YB-16 (*in vivo* mouse PK SubQ). DMPK study was conducted before the *in vivo* efficacy studies. For *in vitro* DMPK, metabolic stability study (time course) was conducted in C57BL6 mouse liver microsome to measure the half-life ($T_{1/2}$) and plasma stability study (time course) was conducted in C57BL6 mouse plasma to measure $T_{1/2}$ (C57BL6 mouse is also used in the efficacy study). YB-2 showed excellent mouse plasma stability with a $T_{1/2}$ of 36 h (2189 min) and two standard control compounds (propantheline and lovastatin) performed as expected in the experiment (Table 3). However, YB-2 was rapidly metabolized by mouse liver microsome with a short $T_{1/2}$ of 3.1 min and the control compound performed as expected in the experiment (Table 4). For *in vivo* PK, single dose of compounds was administered via IV, PO, or SubQ to C57BL6 mice and seven blood samples (20 μL each) were collected per animal in 24 h. Blood samples were analyzed by triple-quad LC/MS/MS. PK parameters were calculated using WinNonlin software. TRPV1 agonist-induced analgesia is related to peripheral action, and no BBB permeability is required. Thus, brain PK has not been tested for our compounds. After YB-2 PO administration (0.4 mg/kg), YB-2 concentrations in mouse plasma were below quantitation limit (1 ng/mL). For IV administration, YB-2 had a short $T_{1/2}$ of 0.17 h (Table 5). The *in vivo* PK data of YB-2 are consistent with the *in vitro* liver microsome stability data. For SubQ administration (2 mg/kg), YB-16 had a $T_{1/2}$ of 1.2 h, much longer than YB-2's $T_{1/2}$ in IV administration. Based on PK data, we prioritized IV and SubQ for systematic administrations instead of PO in addition to intraplantar administration, a common method of TRPV1 modulator delivery. PK formulation [35% *N*-methyl-2-pyrrolidone

https://doi.org/10.1021/acsomega.1c05727
ACS Omega 2022, 7, 2929−2946

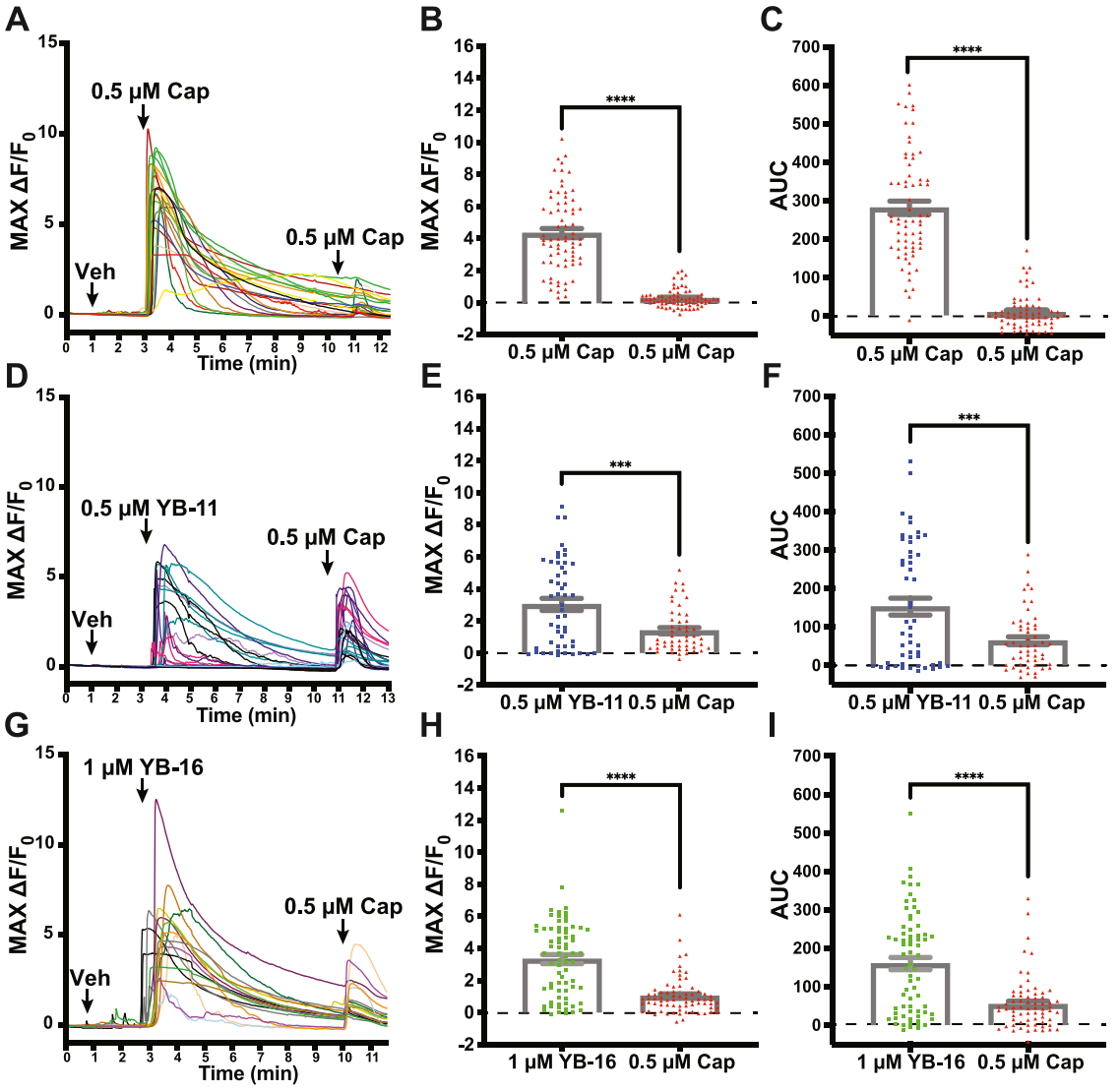

Figure 10. YB-11 and YB-16 on desensitized TRPV1-positive dorsal root ganglion as assessed with *in vitro* Ca^{2+} imaging. (A) Representative traces from an experiment, where dissociated DRG neurons were treated with capsaicin (0.5 μM) approximately 7.5 min before another treatment with capsaicin (0.5 μM). (B) The max Ca^{2+} signal from capsaicin was significantly reduced after the initial capsaicin response. (C) The area under the curve for the Ca^{2+} signal from capsaicin was significantly reduced after the initial capsaicin response. (D) Representative traces from an experiment, where dissociated DRG neurons were treated with YB-11 (0.5 μM) approximately 7.5 min before a treatment with capsaicin (0.5 μM). (E) The max Ca^{2+} signal from capsaicin was significantly reduced after the initial YB-11 response. (F) The area under the curve for the Ca^{2+} signal from capsaicin was significantly reduced after the initial YB-11 response. (G) Representative traces from an experiment, where dissociated DRG neurons were treated with YB-11 (1.0 μM) approximately 7.5 min before a treatment with capsaicin (0.5 μM). (H) The max Ca^{2+} signal from capsaicin was significantly reduced after the initial YB-16 response. (I) The area under the curve for the Ca^{2+} signal from capsaicin was significantly reduced after the initial YB-16 response. Paired *t*-test ***$P < 0.001$, ****$P < 0.0001$. Error bars in panels B, C, E, F, H, I are shown as mean ± SEM.

(NMP) in saline] was used as a vehicle for efficacy studies. PK doses were used to guide the design of dosing parameters for the *in vivo* efficacy experiments.

Determining the Effects of Local YB Compound Administration on Spontaneous Behavior. After building this library of capsaicin analogues, we wanted to test the baseline impact of YB-11 and YB-16 on mouse behavior as well as the analgesic potential of YB-11 and YB-16 in mouse models of acute nociception with either local treatment or systemic treatment.

To determine the immediate effects of the local administration of capsaicin and YB compounds, spontaneous post-treatment behavior was recorded for 120 min after injection. Pain-associated behavior (licking and biting of the right hind paw) was scored in 5 min bins. We completed two separate experiments, one for YB-16 and one for YB-11. For YB-16, male and female mice received a 10 μL intraplantar injection of either vehicle (35% NMP in saline), 10 μg capsaicin, or 5−45 μg of YB-16 to the right hind paw (n = 8−10 per group, equal amounts of males and females). We found significant main effects of time ($P < 0.0001$), treatment ($P < 0.0001$), and time x treatment interactions ($P < 0.0001$) using two-way ANOVA along with several significant multiple comparisons (see Table S1 for statistics; Figure 12A). We also analyzed the total amount of spontaneous behavior for 120 min. We found a significant main effect ($P < 0.0001$) with high-dose capsaicin (10 μg), showing a statistically significant reduction in pain-like behavior compared to that of the vehicle control (P =

https://doi.org/10.1021/acsomega.1c05727
ACS Omega 2022, 7, 2929−2946

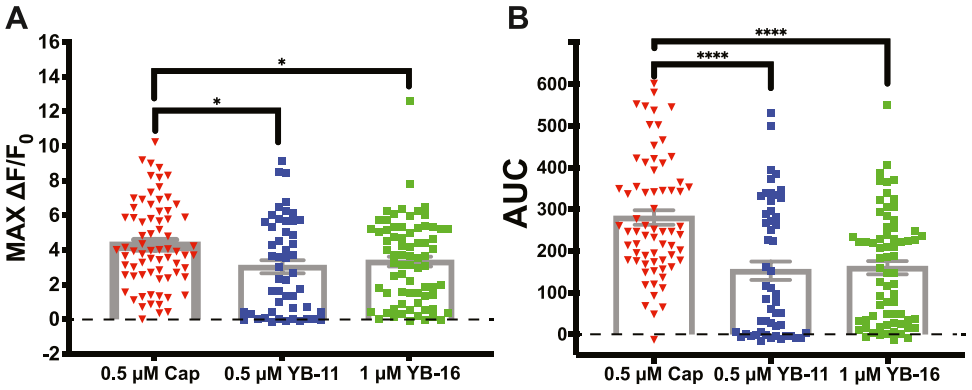

Figure 11. Impact of YB-11 and YB-16 on the dorsal root ganglion Ca^{2+} influx assessed with *in vitro* Ca^{2+} imaging. (A) The max Ca^{2+} signal from YB-11 and YB-16 was significantly reduced compared to that from capsaicin (one-way ANOVA $P = 0.011$). (B) The area under the curve (AUC) Ca^{2+} signal from YB-11 and YB-16 was significantly reduced compared to that from capsaicin (one-way ANOVA $P < 0.0001$). Dunnett's multiple comparison $^*P < 0.05$, $^{****}P < 0.0001$. Data are shown as mean ± SEM.

Table 3. Mouse Plasma Stability

compound	species	concentration (μM)	$T_{1/2}$ (min)	% remaining at T_{120}
YB-2	C57BL6 mouse	2	2189	97
propantheline		5	55	20
lovastatin		5	12	0.2

0.0061; see Table S1 for statistics; Figure 12B). We found that capsaicin (10 μg) causes toxicity, leading to sedation in most of the Charles River C57BL6 mice. Surprisingly, one female mouse died after treatment with 10 μg capsaicin. No adverse behavior was observed for YB-treated mice.

For YB-11, we performed a more limited analysis of spontaneous behavior. Male and female mice received a 10 μL intraplantar injection of either vehicle or 10 μg of YB-11 to the right hind paw (n = 8−10 per group, equal amounts of males and females). We found significant main effects of time ($P = 0.0001$), treatment ($P = 0.012$), and time x treatment interactions ($P = 0.047$) using a mixed-effects model along with a number of statistically significant Sidak multiple comparisons (see Table S2 for statistics; Figure 12C). We also analyzed the total amount of spontaneous behavior for the 120 min trial. We found a statistically significant increase in spontaneous behavior in YB-11-treated mice compared to that of the vehicle control (t-test $P = 0.039$; Figure 12D).

YB-16 and YB-11 Have Antihyperalgesic Effects on Spontaneous Formalin Behavior. Following the paw injections described above, animals were treated in the same paw with formalin to assay behavior in the spontaneous formalin assay. The assay has been used for decades to assess the analgesic effects of various compounds in rodents.[34] In this assay, diluted formalin is injected into the hind paw of the animal and pain-associated behaviors (*e.g.*, licking and biting) are observed over two distinct phases. The first phase (phase I) of the formalin response lasts approximately 10 min and is hallmarked by a robust increase in pain-associated behaviors. After phase I, there is a brief decrease in pain-associated behaviors, followed by a more prolonged second phase (phase II) of pain-associated behaviors lasting from 10 to 60 min.[34,35]

To determine whether YB compounds were able to inhibit formalin-induced nociception, male and female mice received a 10 μL subcutaneous injection of 2% formalin 120 min after the above treatments (vehicle, capsaicin, YB-11, or YB-16). Spontaneous postformalin behavior was recorded for 60 min, and pain-associated behavior (licking and biting of the injected hind paw) was measured in 5 min bins. For YB-16 analysis, two-way ANOVA analysis of 60 min of spontaneous formalin behavior (5 min bins) found a significant main effect of time ($P < 0.0001$), treatment ($P = 0.0072$), and a time x treatment interaction ($P < 0.0001$) using two-way ANOVA along with several significant multiple comparisons (see Table S3 for statistics; Figure 13A). Our results show that all doses of YB-16 tested significantly decreased phase I pain-associated behaviors (Figure 13B). Interestingly, the administration of low-dose YB-16 (5 μg) caused an apparent increase in pain-associated behaviors approximately 20 min post formalin administration (Figure 13A); however, the total amount of pain-associated behavior in phase II did not significantly increase at this dose (Figure 13C). In agreement with previous findings,[11] we found that the positive control capsaicin at 5−10 μg dose was able to reduce the first-phase spontaneous behavior (Figure 13B). The YB-16 (45 μg) treatment group is the only group that showed a statistically significant decrease (54%) in phase II of the formalin test (Figure 13C).

In our analysis of YB-11, we found a significant main effect of time ($P < 0.0001$) but not treatment ($P = 0.3062$) or time x treatment interaction ($P = 0.3999$) using a two-way ANOVA (see Table S4 for statistics; Figure 13D). When evaluating phases I and II of the formalin assay, the administration of 10 μg YB-11 decreased the pain-associated behavior in phase I compared to that of the vehicle control (unpaired t-test $P = 0.0094$; Figure 13D) but not in phase II (unpaired t-test $P = 0.90$; Figure 13F). We intend to test YB-11 at high doses (comparable to 45 μg dose of YB-16) and expect to observe the effect in phase II. Unfortunately, due to the low aqueous

Table 4. Mouse Liver Microsome Stability

compound	species	concentration (μm)	$T_{1/2}$ (min)	% remaining at T_{120}	Cl_{int} (L/(h kg))
YB-2	C57BL6 mouse	2	3.1	0.1	107
Verapamil		2	5	0	65

https://doi.org/10.1021/acsomega.1c05727
ACS Omega 2022, 7, 2929−2946

Table 5. *In Vivo* Mouse PK Summary[a]

compound	species	route	dose (mg/kg)	λz (1/h)	$T_{1/2}$ (h)	T_{max} (h)	C_{max} (ng/mL)	AUC_{last} (hr ng/mL)	MRT (h)
YB-2	C57BL6 mouse	IV	0.4	4.1	0.17	0.083	123	38	0.16
YB-16[b]		SubQ	2	0.59	1.2	0.5	104	173	1.2

[a]λz: the elimination rate constant; AUClast: area under a concentration of analyte vs time calculated from time zero to the time of the last positive *Y* value; and MRT: mean residence time. [b]YB-16 is a prodrug and readily converted into YB-11 *in vivo*; dose (2 mg/kg) was calculated based on YB-11; YB-11 was the target compound in the PK sample analysis.

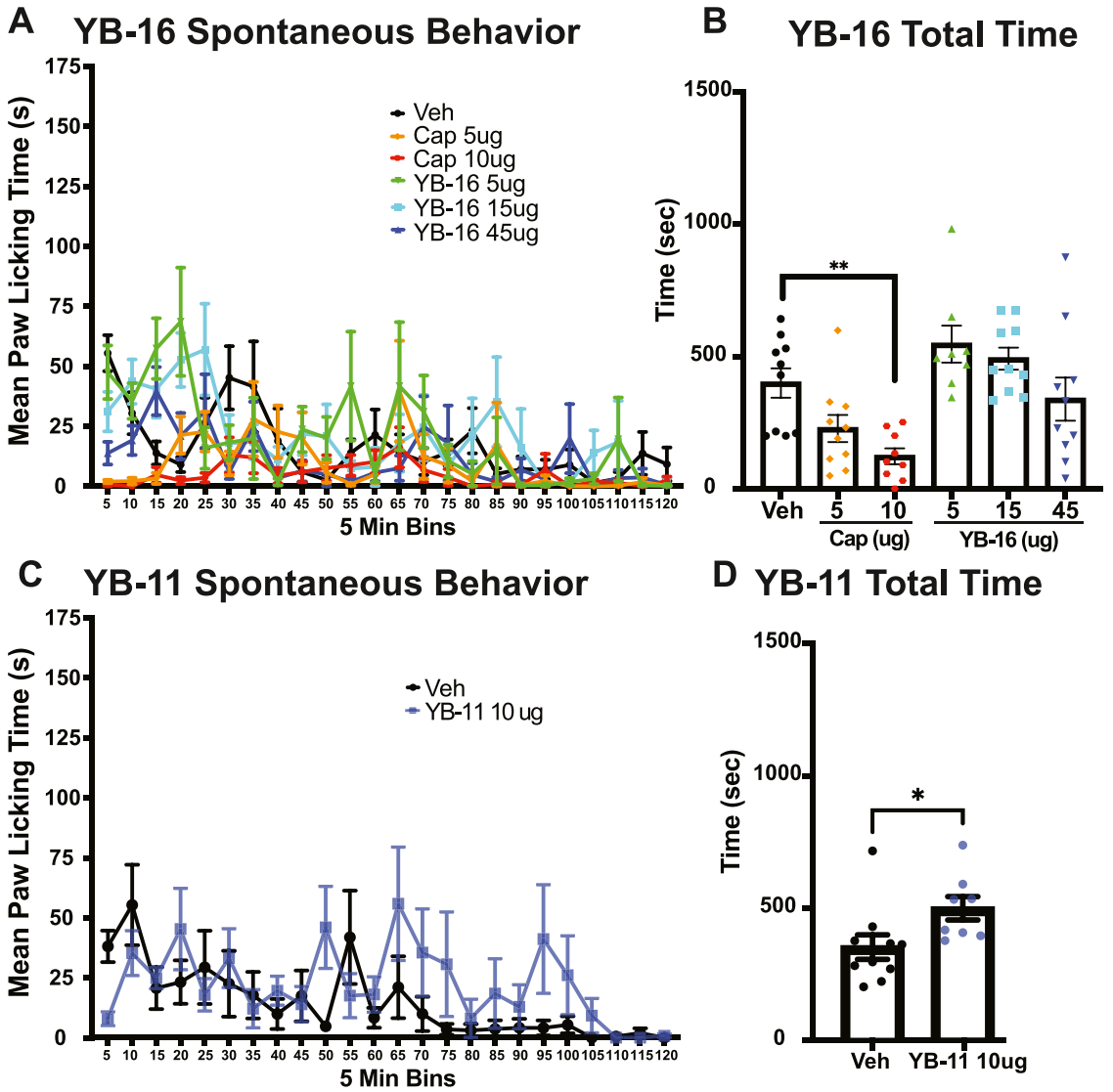

Figure 12. Impact of YB-16 and YB-11 on spontaneous behavior following paw infection. (A) Evaluation of the spontaneous licking and biting of the paw after intraplantar injection of YB-16 (5, 15, 45 μg), capsaicin (5, 10 μg), or vehicle for 120 min after injection (two-way ANOVA $P < 0.001$ main effect treatment, time, and interaction). (B) Total pain-like behavior for YB-16, capsaicin, or vehicle. Capsaicin treatment (10 μg) leads to a significant reduction in pain-like behavior compared to the vehicle control group. (C) Evaluation of the spontaneous licking and biting of the paw after intraplantar injection of YB-11 (10 μg) or vehicle for 120 min after treatment showing main effects of time (mixed-effects model $P < 0.05$ main effect treatment, time, and interaction). (D) Total pain-like behavior for YB-11 or vehicle showing an increase in spontaneous behavior after YB-11 treatment. $^{**}P < 0.01$ Dunnett's multiple comparison. $^{*}P < 0.05$ *t*-test. $n = 8-10$, all groups. Data are shown as mean ± SEM.

solubility of YB-11, we were unable to test the effects of higher doses of YB-11. Due to these solubility limitations of YB-11, and the robust analgesic effects of YB-16 observed in the formalin assay, we decided to not test YB-11 in the following hotplate pain assay.

YB-16 Has Analgesic Effects on Thermal Sensitivity. We next wanted to determine whether YB-16 could reduce pain-associated behavior when administered systemically. Other groups have shown that the systemic administration of 6 mg/kg capsaicin to CD-1 female mice via s.c. injection blocks thermal nociception in the hotplate assay when administered 60 min before testing.[36] We hypothesized that rodents would tolerate higher doses of YB-16 due to its lower pungency (Table 6) and that systemic administration would produce analgesia in the hotplate assay. To this end, we examined the effects of YB-16 on thermal sensitivity in mice using the

https://doi.org/10.1021/acsomega.1c05727
ACS Omega 2022, 7, 2929−2946

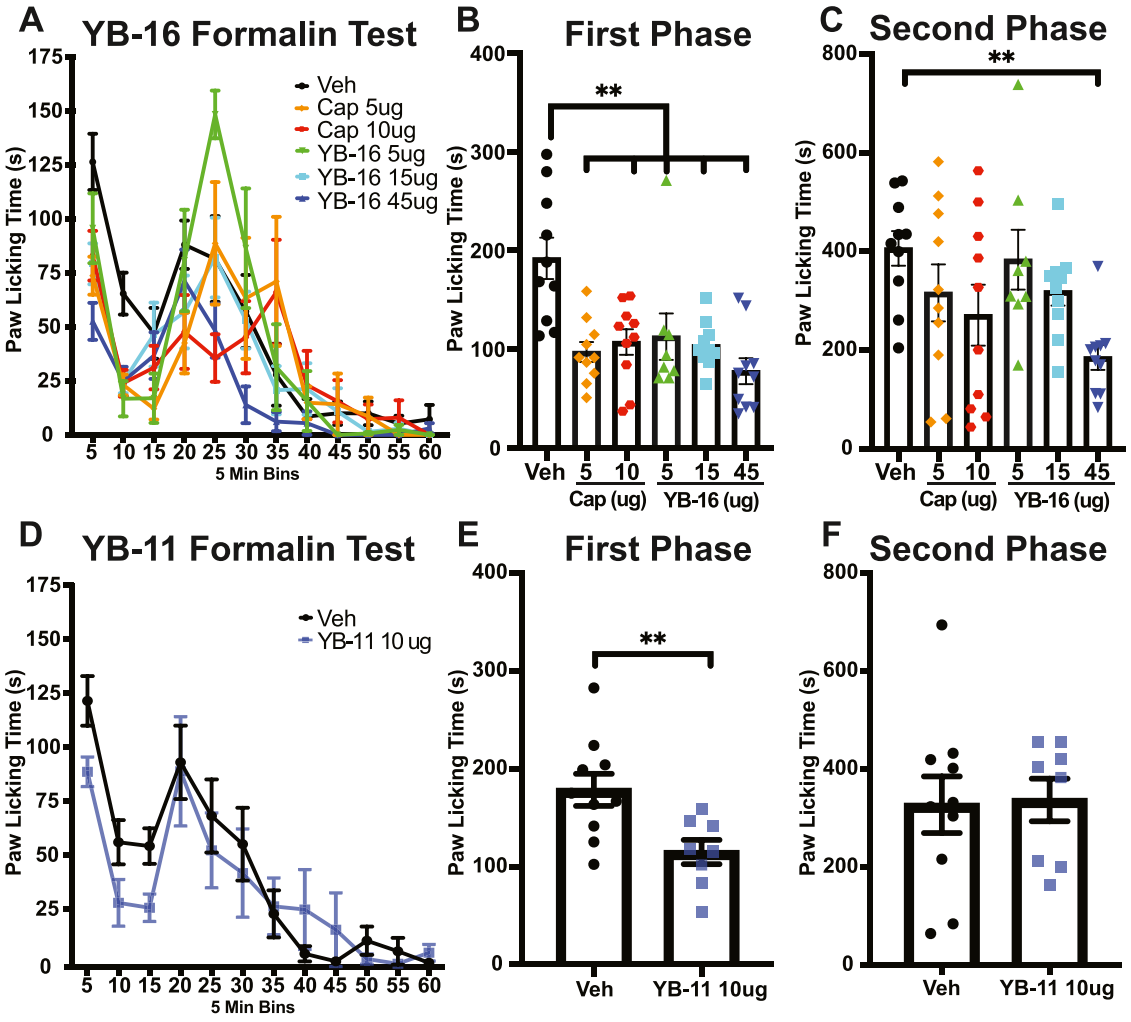

Figure 13. Antihyperalgesic effect of YB-16 and YB-11 on formalin-induced pain. (A) YB-16 (5, 15, 45 μg) and capsaicin (5, 10 μg) reduce the spontaneous pain-like behavior in a dose-related manner (two-way ANOVA $P < 0.01$ main effect treatment, time, and interaction), with significant effects in the (B) first phase (all doses, all treatments) and (C) second phase (45 μg YB-16 only) of the test. (D) YB-11 (10 μg) impact on the spontaneous pain-like behavior (two-way ANOVA $P < 0.01$ main effect time), with significant effects in the (E) first phase but not (F) the second phase of the test. **$P < 0.01$ Dunnett's multiple comparison (B, C) and t-test (E). n = 8−10, all groups. Data are shown as mean ± SEM.

Table 6. Overall Comparison of YB-2, YB-11, YB-16, and Capsaicin

compound	EC_{50} (μM)	solubility (g/l00 mL)	pungency RPP
capsaicin	0.11	0.0013	100
YB-2[a]	0.082	2.0	17.6
YB-11	0.012	0.0027	40.6
YB-16	0.93	0.016	13.6

[a]YB-2 was tested as a HCl salt; RPP, relative pain-producing potency with capsaicin set to 100.

hotplate assay. Male and female mice received subcutaneous injections into the loose skin of the neck consisting of either vehicle, 2 mg/kg capsaicin, 3 mg/kg YB-16, or 6 mg/kg YB-16. Two hours post treatment with drug or vehicle, mice were tested on a hotplate maintained at 49±0.5 °C and the latency to the observation of pain-associated behavior (hind paw lick or jump) was measured. One-way ANOVA found a significant overall main effect of treatment ($P = 0.0098$; see Table S5 for statistics and Figure 14). Multiple comparison Dunnett's tests found that the maximum possible effect (%MPE) of both 2 mg/kg capsaicin ($P = 0.0072$) and 6 mg/kg YB-16 ($P = 0.0213$) was significantly higher than that of the vehicle control (Figure 14). We saw no statistically significant differences in the %MPE of mice treated with 3 mg/kg YB-16 ($P = 0.1336$) compared to that of vehicle, demonstrating that the effects of YB-16 appear to be dose-dependent. Two females treated with 2 mg/kg of capsaicin, a low dose compared to previously published studies,[20,36] died within 5 min of capsaicin administration, causing us to immediately cancel any further capsaicin administration to female mice. Thus, the 2 mg/kg capsaicin-treated group in the hotplate assay is composed of solely male mice.

DISCUSSION AND CONCLUSIONS

Based on our previous experience in modifying natural products,[37,38] three series of capsaicin analogues were carefully designed, synthesized, and tested. Here, we show evidence that the agonist-dependent effect of capsaicin on TRPV1-induced analgesia can be separated from its inherent pungency and hydrophobicity. We designed novel enamide analogue YB-16 by attaching a polar PEG side chain to the aromatic region A, introducing a reverse amide into the linker region B, and replacing the flexible alkyl side chain in the capsaicin region C

https://doi.org/10.1021/acsomega.1c05727
ACS Omega 2022, 7, 2929−2946

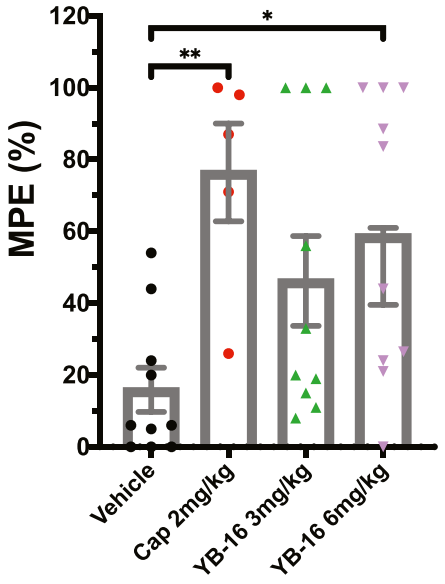

Figure 14. Effect of YB-16 on thermal sensitivity. Subcutaneous systemic injections of capsaicin (2 mg/kg) and YB-16 (6 mg/kg) reduced hotplate sensitivity compared to that of vehicle (one-way ANOVA $P = 0.0098$). $n = 5$ cap group; $n = 10$ other groups. $^{*}P = 0.02$ and $^{**}P = 0.007$ Dunnett's multiple comparison.

with a rigid *trans*-enamide linked with phenyl moiety (Figure 8). YB-16 is a prodrug of YB-11, which showed significantly enhanced TRPV1 potency (YB-11 EC_{50} of 0.012 μM vs capsaicin EC_{50} of 0.11 μM in the Ca^{2+} flux assay).

TRPV1 has a complex polymodal activation profile because it is able to sense multiple stimuli, such as noxious pain, heat, protons, ligand binding, and a number of products of cellular mechanisms.[24,25] Several TRPV1 antagonist candidate drugs have failed in clinical trials because, by interfering with the detection of the aforementioned stimuli, they triggered serious side effects such as hyperthermia and impaired detection of painful heat. Thus, successful TRPV1 modulators need to interfere selectively with only a subset of these activation modalities, leaving the others unperturbed. We have studied the ligand-bounded TRPV1 structures and investigated these ligand:TRPV1 interactions. Structural changes in regions B and C transform the flexible natural product into a rigid compound with a favorable binding conformation, resulting in additional ligand:receptor interactions such as H-bonding with Tyr513 and Arene-H interaction with Leu671 (Figure 7). Ligand rigidification is a proven strategy that is used to improve selectivity for conformationally flexible targets.[39] In analogues YB-16/YB-11, reverse *trans*-enamide linked with aromatic chain effectively rigidifies the flexible natural product, which increases the ligand−receptor interaction, and improves the selectivity and limits the interaction of YB-16/YB-11 with only a small subset of the TRPV1 activation modalities, leaving the others unperturbed. That explains why YB-16/YB-11 are highly effective but less pungent and less toxic in animal models of pain than capsaicin. YB-11 showed an ∼2.4-fold decreased pungency (YB-11 pungency of 40.6 relative pain-producing pungency (RPP) vs capsaicin pungency of 100 RPP) and improved aqueous solubility (YB-11 solubility of 0.0027 g/100 mL vs capsaicin solubility of 0.0013 g/100 mL) (Table 6). PEG-ester side chain on YB-16 is labile in plasma, and YB-16 is readily converted into YB-11 *in vivo* (Table 5). Therefore, YB-16 is a prodrug of YB-11 with decreased pungency (YB-16 pungency of 13.6 RPP vs YB-11 pungency of 40.6 RPP) and improved solubility (YB-16 solubility of 0.016 g/100 mL vs YB-11 solubility of 0.0027 g/100 mL). The amine analogue YB-2 is structurally related to compound 2s in[29] (compared to compound 2s, YB-2 has an olefin and an extra methyl group on the side chain), which was reported to be inactive (>10 μM in the Ca^{2+} influx assay). YB-2 retained the potent TRPV1 activation activity (YB-2 EC_{50} of 0.082 μM vs capsaicin EC_{50} of 0.11 μM), decreased pungency (YB-2 pungency of 17.6 RPP vs capsaicin pungency of 100 RPP), and improved aqueous solubility. For comparison, the YB-2 HCl salt solubility is 2.0 g/100 mL vs sodium phenolate of capsaicin (prepared by treating capsaicin with sodium hydroxide), which has a solubility of 0.10 g/100 mL. These three analogues, in particular, YB-16, are promising candidates that can be further developed into high-impact therapeutic agents.

The synthesis and evaluation of the YB analogues revealed novel insights into the SAR that contradicted some previous reports. We have found that (i) in the aromatic A-region, the phenol group can be replaced with amine or amide groups; (ii) in the amide bond B-region, modification of the secondary amide likely affects the conformation of the molecule, rather than disrupting amide NH from acting as a hydrogen-bonding donor to the TRPV1 receptor; (iii) in the hydrophobic C-region, detailed structural features on the side chain such as electron-withdrawing group or hydrogen bond acceptors have a significant impact on the TRPV1 agonistic activity. The enamide analogues also demonstrated that the introduction of a rigid *trans*-enamide motif in enamide phenol analogues likely provided favorable conformation for TRPV1 binding and increased the potency. However, the introduction of *trans*-enamide motif in enamide amine analogues possibly added desolvation energy required for the aniline and decreased the potency. Introducing polar poly(ethylene glycol) (PEG) substitution on the aniline and phenol analogues resulted in decreased potency. These analogues add to the previously known SAR and provide new insight for *de novo* small-molecule drug design based on capsaicin.

Despite its tremendous medicinal potential, efforts to broaden capsaicin's range of clinical applications have been limited by its high pungency [16 million Scoville Heat Units (SHUs)[40] or 100 RPP] and low aqueous solubility (0.0013 g/100 mL).[41] We were able to alleviate the undesired pungency in capsaicin and improve the aqueous solubility through the following structural modifications: (i) replacing the phenol group with amine (YB-2), (ii) introducing a *trans*-enamide motif (YB-11), and (iii) attaching a polar poly(ethylene glycol) (PEG) side chain to the phenol (YB-16). These three analogues, YB-16, in particular, present an opportunity to treat patients at highly efficacious doses and through a wide range of formulations and routes of administrations.

One of the critical mechanisms by which capsaicin reduces pain signaling is through the desensitization of nociceptors to subsequent noxious stimuli. This desensitization can be observed with *in vitro* Ca^{2+} imaging of DRGs.[32] We found that both YB-11 and YB-16 were able to significantly increase cytosolic Ca^{2+} levels in mouse DRGs and desensitized nociceptors. Consistent with the EC_{50} data acquired from transiently transfected HEK-293 cells, higher concentrations of YB-16 were required to both activate and desensitize nociceptors. Despite the lower EC_{50} of YB-11 compared to that of capsaicin in HEK-293 cells overexpressing human TRPV1, YB-11 produced smaller changes in intracellular Ca^{2+}

https://doi.org/10.1021/acsomega.1c05727
ACS Omega 2022, 7, 2929−2946

than capsaicin in mouse nociceptors at equal concentrations, suggesting potential species differences. Furthermore, both YB-11 and YB-16 desensitized a smaller population of TRPV1+ neurons compared to the capsaicin-positive control. Since cytosolic Ca^{2+} has been shown to be critical for the desensitizing effects of capsaicin,[12,33] the reduced ability of YB analogues to increase intracellular Ca^{2+} levels compared to that of capsaicin could explain the observed decreases in mouse nociceptor desensitization. Nevertheless, the *in vitro* data in mouse DRGs do demonstrate that both compounds are able to desensitize nociceptors despite the modifications made to the aromatic region, amide region, and hydrophobic change of the capsaicin structure.

We found that the local administration of YB-11, but not YB-16, caused a transient increase in spontaneous pain-like biting and licking when delivered into the right hind paw. These data fit with the observed reduced pungency of YB-16. Somewhat surprisingly, mice treated in the paw with higher doses of capsaicin showed a reduction in spontaneous behavior compared to vehicle-treated mice. These data stand in contrast to studies demonstrating that the intraplantar administration of 10 μg of capsaicin increases in spontaneous pain-like response.[9] We hypothesize that 10 μg in our hands causes toxicity, leading to sedation in most of the Charles River C57BL6 mice.

Our results demonstrate that lower doses of YB-11 and YB-16 are effective at reducing pain-associated behavior in the first phase of the formalin assay, but higher doses are required to significantly reduce pain-associated behavior in the second phase. Two distinct mechanisms are responsible for the biphasic distribution of pain-associated behavior in the formalin assay.[35,42] The first phase of the formalin response is mediated by the direct activation of TRPA1 receptors on nociceptors,[42] while the second phase is likely mediated by the sensitization of neurons in the dorsal horn of the spinal cord.[35] It is possible that the local administration of TRPV1 agonists is more effective at desensitizing nociceptors to the direct activation of TRPA1 than at inhibiting central sensitization. We plan to assess the PK of YB-11 and YB-16 vial local administration to confirm this hypothesis in the future. This is likely because higher concentrations of TRPV1 agonists are needed to penetrate, and defunctionalize, enough nociceptive fibers to prevent this plasticity. This also supports the hypothesis that while desensitization of receptors on nociceptive afferents may occur relatively quickly, sustained increases in intracellular Ca^{2+} are required for the full defunctionalization of nociceptive neurons.[13,21]

Curiously, others have reported that the same dose of capsaicin (10 μg into the hind paw, 2 h before the administration of formalin) reduced the pain-associated behavior in both phases of the formalin assay in C57BL/6J mice.[9] It may be that there are physiological differences between the Charles River C57BL/6 mice used here and those sourced from the Jackson Laboratory, which could explain these contradicting results, including differences in TRPV1 expression or distribution. However, the evaluation of such strain differences was outside of the scope of this study.

In cases where patients experience pain in several regions of the body, the local administration of analgesics may not be practical. Systemic administration of capsaicin is not a viable clinical strategy due to the toxic side effects associated with this form of drug administration including tachycardia and severe hypotension.[20,43] In this study, the systemic administration of YB-16 via s.c. injection had a dose-dependent effect on thermal sensitivity in the hotplate assay. No deleterious side effects of YB-16 injection were observed in this study. Capsaicin also reduced thermal sensitivity in male mice. Surprisingly, two female Charles River C57BL/6 mice died within minutes of administration of 2 mg/kg capsaicin, preventing us from continuing with the testing of this experimental group. Lower doses of capsaicin will be tested in future experiments. Yet, all male mice survived capsaicin administration. Previous reports have estimated the LD_{50} of capsaicin via s.c. administration to be 9 mg/kg in mice.[20] Furthermore, 6 mg/kg of capsaicin increased latency in the hotplate assay in CD-1 female mice, without any reported lethality.[36] In addition, another female mouse spontaneously seized following intraplantar capsaicin (10 μg). The animal died within 2−15 min of intraplantar capsaicin treatment. Another female animal receiving 10 μg capsaicin displayed significant sedation (no movement for ∼20 min after capsaicin dosing) but did recover and had stereotyped formalin behavior.

Still, as scientists begin to expand their studies of female physiology, sex differences in the pharmacology and toxicology of many drugs have been revealed.[44] Indeed, recent studies suggest that sex differences in the expression of drug-metabolizing enzymes, expression of transporters, and the direct influence of reproductive hormones on drug targets, among other physiological differences between the sexes, are responsible for the propensity of females to experience greater adverse drug effects compared to those of their male counterparts.[44] Clearly, more research is needed to explore the sex differences in even "well-established" pharmacological agents. Due to the surprising nature of these results, the determination of the mechanisms behind these sex differences was outside of the scope of this study. It is important to note that all female mice treated with YB-16 (intraplantar and s.c.) and YB-11 (intraplantar) survived, and no deleterious side effects were observed. This supports our hypothesis that nonpungent capsaicin analogues produce less deleterious side effects *in vivo* and that nonpungent TRPV1 agonists may not be limited to local administration with suboptimal low doses.

We aim to carry out additional studies to determine the safety and efficacy of YB-16 as an analgesic and to determine if YB-16 has sufficient therapeutic window and analgesic effectiveness to warrant further development as a clinical candidate. The use of TRPV1 modulators as analgesics remains controversial due to the adverse side effects observed in clinical trials.[45] Yet, it is clear that TRPV1 modulation does significantly reduce nociception and is a viable target for the alleviation of many types of pain.[5,10,13,45] The challenge of identifying and synthesizing safe and effective TRPV1 modulators remains, but we remain hopeful that the increased understanding of the SAR of capsaicin may lead to the generation of compounds that can induce the defunctionalization of nociceptors without harmful side effects. By eliminating the limitations caused by high pungency and solubility, the dosages of candidate drugs used in clinical trials can be increased to match preclinical tests. Thus, it will be much easier to achieve therapeutic end points.

EXPERIMENTAL SECTION

Design and Synthesis of YB TRPV1 Agonists. To explore the structure−activity relationship (SAR) of capsaicin, we designed analogues to explore modifications of the aromatic

https://doi.org/10.1021/acsomega.1c05727
ACS Omega 2022, 7, 2929−2946

region (Figure 2A), the amide region (Figure 2B), and the hydrophobic side chain of capsaicin (Figure 2C).

To synthesize the amine series of analogues, (6*E*)-8-methyl-6-nonenoic acid (MNA; Labnetwork) was coupled with 4-(aminomethyl)-2-methoxyaniline (Enamine), using hexafluorophosphate azabenzotriazole tetramethyl uronium (HATU), to prepare the diacylated (YB-1) and monoacylated (YB-2) analogues (Figure 3A) (see Scheme S1 for documentation for synthesis; see Table S6 for SMILES formulas for YB compounds). YB-2 was then treated with methanesulfonyl chloride (MsCl), in the presence of triethylamine (Et_3N) to produce the monomesylated (YB-6) and dimesylated (YB-7) analogues. The aniline of YB-2 can be methylated using paraformaldehyde under acidic conditions, followed by reduction with sodium borohydride to furnish the N-methylated YB-8 analogue. Acetylation of YB-2 with acetic acid using HATU afforded N-acetyl YB-9. Pegylated analogue YB-13 could be made in one-pot by coupled MNA with AMA using HATU, followed by treatment with m-PEG3-acid (Broadpharm).

To synthesize the oxazoline series of analogues, homovanillic acid (Enamine) was first protected with tert-butyldimethylsilyl chloride (TBS-Cl) in the presence of Et_3N to prepare TBS-homovanillic acid (THA) (Figure 3B). THA was then coupled with different amino alcohols using HATU to generate β-hydroxyamide intermediates, which was then treated with MsCl and Et_3N to provide mesylated intermediates. The mesylate was reacted with 1,8-diazabicyclo [5.4.0] undec-7-ene (DBU) to form the oxazoline ring, followed by tetrabutylammonium fluoride (TBAF) to deprotect the phenol in one-pot to afford analogues YB-3, YB-4, and YB-5.

To synthesize the enamide series of analogues, THA was coupled with hydroxylamine hydrochloride (Thermo Fisher Scientific) using HATU to prepare the hydroxyamide intermediate, which was further treated with pivaloyl chloride (Piv-Cl) and Et_3N to produce pivaloyloxyl amide (Figure 3C). The pivaloyloxyl amide was then subjected to rhodium-catalyzed cross coupling with *trans*-2-(4-chlorophenyl) vinylboronic acid (Thermo Fisher Scientific) in the presence of sodium acetate and a catalytic amount of pentamethylcyclopentadienyl rhodium dichloride followed by TBAF deprotection to afford YB-10.[31] A similar procedure using different vinylboronic acids was used to prepare YB-11, 12, 14, 15, 22, and 23. The vinylboronic acid reagents were either purchased from commercial sources or prepared from their respective alkynes.[31] Pegylated analogue YB-16 was made by treating YB-11 with a mixed anhydride prepared from Piv-Cl and m-PEG3-acid. To make aniline derivatives, hydroxylamine hydrochloride was first protected with Boc anhydride (BOC_2O) to prepare *N*-Boc-hydroxylamine, which was reacted with Piv-Cl and treated with TFA to produce the TFA salt of pivaloyloxyl amine. AMA was protected with 9-fluorenylmethoxycarbonyl chloride (Fmoc-Cl) before being coupled with pivaloyloxyl amine TFA salt using HATU to provide the pivaloyloxyl amide intermediate. The pivaloyloxyl amide was then coupled with *trans*-2-[4-(trifluoromethyl) phenyl] vinylboronic acid (Combi-Blocks) using the same rhodium-catalyzed cross coupling used previously, followed by piperidine treatment to remove the FMOC and afford YB-17. A similar procedure with different vinylboronic acids was used to prepare analogues YB-18, 19, 20, and 21.

Based on early *in vitro* results, it was determined that larger amounts of YB-2, YB-11, and YB-16 would be required for additional *in vitro* and *in vivo* experiments. To improve the yield of the YB-2 synthesis, MNA was allowed to couple with a slight excess of AMA using HATU to produce YB-2 resulting in a 96% yield (Figure 4). To improve the yield of the YB-11, THA was coupled with pivaloyloxyl amine TFA salt rather than Piv-Cl using HATU to generate the pivaloyloxyl amide intermediate (Figure 4). NMR analysis showed that the pivaloyloxyl amide prepared using this method had higher purity than the material prepared using the previous method described above (Figure 3C). Pivaloyloxyl amide was coupled with *trans*-2-[4-(trifluoromethyl)phenyl] vinylboronic acid in the same manner as before to afford YB-11 (68% yield). YB-11 was treated with the mixed anhydride prepared from Piv-Cl and m-PEG3-acid to produce YB-16 (43% yield) similarly to the previously mentioned synthesis.

Nuclear Magnetic Resonance (NMR) and Purification. Intermediates and final analogues were analyzed by a JEOL 400 MHz NMR ($CDCl_3$) to verify the chemical structures of the compounds synthesized and were analyzed by a Waters Acquity UPLC with an SQD Mass Spec (Acquity UPLC BEH C18 1.7 μm 2.1mm × 50 mm column, Part No. 188002350; 5−95% acetonitrile−water gradient with 0.1% formic acid) to determine their purity. Final compounds were purified by silica gel chromatography to achieve high purity (>95% based on HPLC analysis) (see Figure S1 for YB-11 and YB-16 HPLC, MS, UV data).

Overexpression of TRPV1 in HEK-293 Cells. The plasmid DNA carrying the human TRPV1 coding sequence (GenScript Biotech Corp, Piscataway, NJ) was introduced into *Escherichia coli* DH5α-competent cells (Invitrogen) to prepare large-scale plasmid DNA (Figure 5A). The plasmid DNA was purified using the Purelink Expi Endodoxin-Free Maxi plasmid purification kit (Invitrogen). The quality and quantity of the plasmid DNA were determined by OD260 and OD280 on a VWR UV-1600PC spectrophotometer. The plasmid DNA was further visualized on agarose gel stained with ethidium bromide with an α Innotech Fluor Chem system. Human embryonic kidney (HEK-293) cells (Invitrogen) were transiently transfected with plasmid DNA for 18−23 h. Western blot was used to confirm the TRPV1 expression in cells (Figure 5B).[28,46,47] It was determined that 23 h was the optimal time for transfection.

After 23 h, the transfected cells were harvested. The cell pellet was resuspended in the freezing medium containing 10% DMSO at a concentration of 11 million cells/mL. One milliliter of cells was distributed into each cryovial. The transfected cells were slowly frozen in a -80° C freezer and then stored in liquid nitrogen until screening use.

Ca^{2+} Flux *In Vitro* Screening. A high-throughput cell-based Ca^{2+} flux assay was established in a 96-well format using the TRPV1 overexpressed cells pretreated with calcium dye (Molecular Device, San Jose, CA).[31−33] After the addition of test compounds, the fluorescence signals were read on a fluorometric imaging plate reader (Synergy H1 Multi-Mode Reader, BioTek Instruments, Inc., Winooski, Vermont). Capsaicin (1 μM; Matrix Scientific) was used as a positive control for the assay. A 3 min kinetic reading protocol with blank subtraction was set up using Gen5 software. The excitation wavelength was set at 485 nm, and the emission wavelength was set at 525 nm. After the initial background reading, compound solutions were added to the plate with a multichannel pipette and the 3 min kinetic reading started immediately. The maximum value for each kinetic reading was

https://doi.org/10.1021/acsomega.1c05727
ACS Omega 2022, 7, 2929−2946

subtracted by the background value of the same well to give the net value. Then, the net values were plotted against the corresponding concentrations to generate dose−response curves and the EC_{50} for each compound was calculated.

Animals. To produce Nestin-GCaMP6f transgenic mice for Ca^{2+} imaging, we crossed C57Bl/6J mice (Jackson Laboratories, Bar Harbor, ME) expressing a Cre-dependent GCamp6f calcium sensor B6J.Cg-*Gt(ROSA)-26Sor*$^{tm95.1(CAG-GCaMP6f)Hze}$/MwarJ (JAX #028865)[48] with C57Bl/6J mice containing a Nestin promoter-driven Cre recombinase, B6.Cg-Tg(Nes-cre)1Kln/J (JAX #003771).[49,50] The resulting offspring were genotyped using commercially available primers from Integrated DNA Technologies, Inc. Male mice of over 45 days of age that were heterozygous for the GCamp6f gene and positive for Nes-Cre recombinase were used for all fluorescent imaging experiments.

Assays were conducted using male and female C57BL/6 mice (Charles River Laboratory, Wilmington, MA) aged 7−9 weeks (formalin and hotplate tests) or 18−20 weeks (pungency). Mice were allowed to acclimate in the housing facility for >5 days after arrival in cages with three to four mice prior to use. The animals were housed in 12 h light/dark cycles with ad libitum access to food and water. All protocols and procedures were conducted according to protocol 1909-10 (Duquesne University) or 20-04 (University of Texas at Dallas) and were approved by the relevant Institutional Animal Care and Use Committees.

Ca^{2+} Flux Assays in Primary Mouse Sensory Neurons. *Preparation of Primary Mouse Sensory Neuron Cultures from Dorsal Root Ganglia (DRG).* Twelve millimeter glass coverslips were coated with 80 μL of a 0.05 mg/mL poly-D-lysine (PDL) and 0.02 mg/mL mouse laminin (Sigma-Aldrich) and incubated at 37 °C overnight. Coverslips were rinsed with autoclaved ddH_2O and dried at room temperature in a laminar flow hood.

Nestin-GCaMP6f transgenic male mice were decapitated, and the spinal column was removed and placed in ice-cold Hanks balanced salt solution (HBSS, Life Technologies) supplemented with 10 mM HEPES (Life Technologies). The removal, dissociation, and trituration of dorsal root ganglia (DRG) were performed in HBSS/HEPES unless otherwise noted. DRGs from the thoracic, lumbar, and sacral regions were removed and dissociated via enzymatic digestion with 15 IU/mL papain (Worthington Biochemical) and 2.25 mg/mL collagenase (Sigma-Aldrich) at 37 °C for 20 min. DRGs were then rinsed with HBSS/HEPES and resuspended in approximately 2 mL of warm media containing 100 μg/ DNAse (Sigma-Aldrich). DRGs were then triturated with fire-polished glass pipettes; the resulting suspension was filtered through a 40 μm Nylon cell strainer (Falcon). The filtered cell suspension was centrifuged at 160 rcf for 4 min, washed, and pelleted again. The cell pellet was resuspended in supplemented neurobasal A media containing the following: neurobasal A media (Thermo Fisher), 5% HI FBS (Sigma-Aldrich), B-27 (Thermo Fisher), 2 mM GlutaMax-1 (Thermo Fisher), and 50 IU/mL penicillin/streptomycin (Thermo Fisher). Cells were plated onto PDL/laminin-coated 12 mm glass coverslips and incubated at 37 °C in supplemented neurobasal A media. Cells were imaged 24−48 h post plating.

Fluorescent Imaging. Fluorescent images were acquired using Cell-Sense software (Olympus) on a BX51WI upright microscope (Olympus) equipped with a 480 nm interface filter, a 505 nm dichroic mirror, and a 535 nm barrier filter (FITC band-pass filter cube, Olympus) and an Orca Fusion C14440 sCMOS camera (Hamamatsu). Two images were captured per second to monitor the relative changes in intracellular Ca^{2+} over time.

Compound Application. All compounds and vehicles were dissolved into the recording solution containing the following: 140 mM NaCl, 5 mM KCl, 2.6 mM $CaCl_2$, 1 mM $MgCl_2$, and 0.56% w/v glucose (Sigma-Aldrich); the pH was adjusted to 7.40 using Trizma-base (Sigma-Aldrich). Compound and vehicle solutions were applied to neurons by bath using a switching valve system (VC-6, Warner Instruments) into a 358 μL chamber (Warner Instruments, RC-21B). The flow rate into the chamber was controlled with a pressurized system (VPP-6, Warner Instruments) using nitrogen gas. For desensitization experiments, cells were allowed to recover for 7−7.5 min between compound applications. KCl (60 mM) was applied at the end of the recording as a positive control for neuronal activation. For Ca^{2+} imaging in DRG neurons, capsaicin and YB compound solutions were made by diluting from stocks (DMSO) into the recording solution to a final concentration of 0.5−1.0 μM of compound. A vehicle control recording solution of 0.05% DMSO v/v was applied to all cells before the application of TRPV1 compounds; cells that responded to vehicle were excluded from the study. Two experiments were completed (n = 2 male Nestin-Cre-GCaMP6f mice). In a pilot experiment (data not shown), doses of capsaicin, YB-11, and YB-16 were evaluated for their ability to induce a change in intracellular Ca^{2+} indicative of TRPV1 activation. The capsaicin concentration (0.5 μM) was chosen from the literature based on its ability to show desensitization with multiple treatments in DRG neurons and pilot studies.[32] We found that DRG neurons were sensitive to capsaicin and 0.5 μM YB-11 but not to 0.5 μM YB-16. In the confirmatory experiment (data shown), the dose of YB-16 was increased to 1 μM. In that experiment, two coverslips were tested for each experimental combination, which was set up as a double treatment paradigm. Cells were first treated with capsaicin/compound ∼7.5 min prior to a second treatment with capsaicin. The full set of combinations tested included 0.5 μM capsaicin/0.5 μM capsaicin, 0.5 μM YB-11/0.5 μM capsaicin, and 1.0 μM YB-16/0.5 μM capsaicin experiments. Individual TRPV1-sensitive neurons were analyzed in statistical analyses across the two coverslips. We evaluated the max Ca^{2+} signal and area under the curve to the first treatment (metric of the total acute TRPV1 activation) as well as the max Ca^{2+} signal and area under the curve to the second treatment (metric of TRPV1 desensitization caused by the first treatment). Additional analysis details can be found in the Statistics section.

Pungency Test of YB TRPV1 Agonists. The original pungency assay for capsaicin and related compounds is the human physiological Scoville scale method.[51] This test measures the highest dilution of a compound at which the pungency (spiciness or "heat") could be detected, as recorded in Scoville Heat Units (SHUs). However, modern analysis of capsaicinoids uses HPLC for natural compound concentration in foods or animal-based assays to avoid potential harm to human volunteers. Here, we used the rodent eye wiping assay.[52−55] Briefly, 5 μL of vehicle (20% Tween-80 in saline) or dilute compound (capsaicin 0.01, 0.1, 0.25, 1 mg/mL; YB-2 0.01, 0.1, 1 mg/mL; YB-11 0.01, 0.1, 1 mg/mL; YB-16 0.1, 0.25, 1, 1.5 mg/mL in vehicle) was gently pipetted into the left or right eye of a male or female mouse (equal numbers used).

https://doi.org/10.1021/acsomega.1c05727
ACS Omega 2022, 7, 2929−2946

Mice were then placed in a 4 cm × 11 cm × 10 cm ventilated Plexiglas arena for 2 min. Mice were recorded by two smartphones (IPhone X, Apple) at 120 frames per second. The number of single forearm wipes to the dosed eye was measured across the first minute of the trial by an experimenter blinded to treatment and experimental hypothesis. Following recording, the eye was flushed by saline. In pilot studies, no wiping was observed at the highest capsaicin dose (1 mg/mL), 5 min after application. All wipe values were normalized to the control vehicle group (n = 6; 10.125 + 1.88 SEM wipes) by subtracting the vehicle mean from measured wipes for each individual trial. The dose that produced 10 normalized wipes was defined as the moderate pain-producing potency (MPP) for capsaicin and all YB compounds. The MPP for capsaicin was set to a relative pain-producing potency of 100, and YB MPP values were used to calculate YB RPP values. A wash-out period of >3 days was used between retesting any individual mouse.

Behavioral Testing. *Drugs and Dosing.* Capsaicin (8-methyl-*N*-vanillyl-6-nonenamide) was purchased from Sigma-Aldrich (St. Louis, MO). Dosing of capsaicin (positive control) for *in vivo* testing was determined from the existing literature on capsaicin-induced analgesia in animal models and adapted to our experimental setup.[9] Dosing estimations for YB compounds were guided by PK data (data not shown) and by comparing *in vitro* agonistic activity in the Ca^{2+} flux assay to capsaicin. Capsaicin and YB compounds were all dissolved in vehicle (35% *N*-methyl-2-pyrrolidone (NMP), 65% saline) at the indicated concentrations (see the Results section) prior to *in vivo* administration.

Drug Delivery Routes. For the spontaneous formalin assays, either capsaicin, experimental compounds, or vehicle control were delivered via 10 μL subcutaneous injections in the right hind paw during light restraint. For the hotplate studies, compounds were administered to mice systemically via 40−50 μL subcutaneous injection at the nape of the neck. All injections were performed by an experimenter blinded to treatment.

Experimental Design. Formalin and hotplate behavioral experiments were designed using the U.K.-based 3R's experimental design assistant system (https://www.nc3rs.org.uk/experimental-design-assistant-eda). This allowed for *a priori* determination of the blinding process and randomization of animals to experimental groups. A power analysis using an α factor of 0.05, a power of 0.90, and expecting an effect size of 1.4−1.8 indicated that groups of 6−12 mice should be sufficient to detect significant effects as small as 1 standard deviation. For behavioral experiments, group sizes of 8−10 animals were used (equal male and female planned). All experimenters were blinded to treatment during drug administration, scoring, and data analysis.

Spontaneous Formalin Test. Adult male and female mice were placed in observation cages (11 cm × 11 cm × 16.5 cm) on a clear plexiglass platform (96 cm × 36 cm × 46.5 cm) and allowed to habituate to the room and the testing apparatus for a total of 60 min prior to drug or vehicle administration. White noise at 60 dB was played during habituation and for the duration of the experiments. A camera (Logitech C910) was placed underneath the clear plexiglass platform to record spontaneous behavior. Immediately following the habituation period, 10 μL of either vehicle or drug (capsaicin, YB-11, or YB-16 totaling between 5 and 45 μg) was administered subcutaneously to the right hind paw of the animal. Mice were returned to their observation cages and recorded for 120 min prior to formalin administration.

A 2% formalin solution was made by diluting formalin (Sigma-Aldrich, 37% formaldehyde in water) in saline. All mice then received a subcutaneous injection of 10 μL of formalin solution into the right hind paw and were subsequently returned to their observation cages for an additional 60 min. Animals were recorded continuously from the point of drug or vehicle administration to 60 min post formalin administration. All recordings were conducted with either Logitech or Windows 10 Camera software. Spontaneous behavior (after the initial drug or subsequent formalin injection) was scored by measuring the total time of right hind paw licking or biting within 5 min bins using a stopwatch.

Hotplate Thermal Assay. The hotplate apparatus consisted of a 10 cm × 16 cm thermoelectric plate (TE Technology CP-061HT) connected to a temperature controller (TE Technology TC-48-20). A mobile, transparent, and colorless plexiglass rectangular prism (10 cm × 16 cm × 25 cm) was placed on the hotplate to form the observation area. The temperature of the hotplate was monitored at all times. Adult male and female mice first received acclimations to the hotplate apparatus set to a non-noxious temperature (one trial 30 min prior to the baseline test and two acclimation trials 24 h before test day). Acclimation trials were on the metal hotplate maintained at 30 ± 0.5 °C (non-noxious temperature) for approximately 60 s per trial. Following acclimation, baseline tests (at least 48 h before drug or vehicle administration) and post-treatment hotplate tests (2 h post drug or vehicle administration) were performed. For the baseline and post-treatment tests, the metal hotplate was maintained at 49 ± 0.5 °C. Measurements were made by placing one mouse on the hotplate at a time and recording the response latency with a stopwatch to the nearest 0.01 s. A cutoff latency of 30 s was used. Pain-associated behavior responses were characterized by either licking of the hind paw or jumping. After each measurement, the plate was wiped clean of all urine and feces. At least 48 h after the baseline hotplate measurement, and 24 h after receiving two additional acclimation trials, mice received a 40−50 μL subcutaneous injection on their dorsal side of either vehicle (35% NMP, 65% saline), 2 mg/kg capsaicin, 3 mg/kg YB-16, or 6 mg/kg YB-16. The maximum possible effect (%MPE) of treatment was calculated using the following formula: $\%\,\mathrm{MPE} = \frac{\text{test day (s)} - \text{baseline (s)}}{30\ \text{s} - \text{baseline}} \times 100\%$. All experimenters were blinded to treatment during testing, scoring, and data analysis.

Statistics. GraphPad Prism (version 8.0) was used for all statistical analysis. Capsaicin and YB compounds were tested three times in the Ca^{2+} flux assay. EC_{50} data are shown as mean ± SEM (Table 1). For the DRG Ca^{2+} experiments, the changes in fluorescence over time ($\Delta F/F_0$), the peak fluorescence post drug application (max $\Delta F/F_0$), and area under the curve (AUC) post drug application were calculated using a custom MatLab program. ROIs that had a max $\Delta F/F_0 \geq 0.3$ to any of the TRPV1 agonists applied were considered "responsive" cells; unresponsive cells were excluded from further analysis. The total number of cells that responded to one or both agonists, and the magnitude of these responses, was analyzed to determine the total number of desensitized TRPV1-positive neurons. The magnitudes of the first and second drugs were analyzed using a paired t-test. The max $\Delta F/F_0$ and AUCs of the first application of capsaicin, YB-11, and YB-16 were

https://doi.org/10.1021/acsomega.1c05727
ACS Omega 2022, 7, 2929−2946

compared to one another using a one-way ANOVA with Dunnett's post hoc multiple comparison test.

As described above, eye wipe behavior was normalized to vehicle control. The mean normalized eye wipes per concentration of drug were then determined; curves of best fit were calculated using an agonist-response (three-parameters) nonlinear regression model (GraphPad Prism version 8.0).

Spontaneous behavior following the initial drug/vehicle injection was analyzed with two methods: (1) analysis in 5 min bins across the 120 min after injection. For YB-16, data were analyzed using repeated-measures two-way ANOVA with Tukey's post hoc multiple comparisons. For YB-11, a mixed-effects model followed by Sidak's post hoc multiple comparisons was used. A mixed-effects model was used due to missing data bins based on a limited random video recording failure. All of the failed bins (one 5 min bin per mouse; 3 mice per group) occurred in the second hour of assay typically in the period where most animals were fully at rest. This mixed model uses a compound symmetry covariance matrix and is fit using restricted maximum likelihood (REML). In the absence of missing values, this method gives the same *P* values and multiple comparison tests as repeated-measures ANOVA. In the presence of missing values (missing completely at random), the results can be interpreted like repeated-measures ANOVA. (2) In addition, the total spontaneous behavior was summed up over the full 120 min. Data were analyzed with one-way ANOVA with Dunnett's multiple comparison test comparing all groups to the vehicle control group for YB-16 and unpaired two-tailed *t*-test for YB-11.

Spontaneous behavior following formalin injection was analyzed using two methods: (1) data in 5 min bins were analyzed with repeated-measures two-way ANOVA followed by Tukey or Sidak multiple comparisons. (2) The first (0−10 min) and second (10−60 min) phases of formalin behavior were separately analyzed for YB-16 using one-way ANOVAs followed by Dunnett's post hoc multiple comparisons of all groups to the vehicle control group or for YB-11 using an unpaired two-tailed *t*-test. Results from the hotplate behavior were analyzed using one-way ANOVA followed by Dunnett's post hoc multiple comparisons of all groups to the vehicle control group. Data are shown as mean ± SEM. *P* values less than 0.05 were considered statistically significant.

■ ASSOCIATED CONTENT

Supporting Information

The Supporting Information is available free of charge at https://pubs.acs.org/doi/10.1021/acsomega.1c05727.

Supporting documentation for synthesis (Scheme S1); YB-11 and YB-16 HPLC, MS, and UV data (Figure S1); Figure 12A,B statistics (Table S1); Figure 12C,D statistics (Table S2); Figure 13A−C statistics (Table S3); Figure 13D−F statistics (Table S4); Figure 14 statistics (Table S5); SMILES formulas for YB compounds (Table S6) (PDF)

■ AUTHOR INFORMATION

Corresponding Authors

Benedict Kolber − *Department of Neuroscience and Center for Advanced Pain Studies, University of Texas at Dallas, Richardson, Texas 75080, United States;* orcid.org/0000-0001-8665-1805; Email: Benedict.Kolber@utdallas.edu

Young Shen − *Young BioPharma, LLC, Lowell, Massachusetts 01852, United States*; Email: yshen@youngbiopharma.com

Authors

Anny Treat − *Department of Neuroscience and Center for Advanced Pain Studies, University of Texas at Dallas, Richardson, Texas 75080, United States*

Vianie Henri − *Department of Biological Sciences, Duquesne University, Pittsburgh, Pennsylvania 15282, United States; Graduate School of Pharmaceutical Sciences, Duquesne University, Pittsburgh, Pennsylvania 15282, United States*

Junke Liu − *Young BioPharma, LLC, Lowell, Massachusetts 01852, United States*

Joyce Shen − *Young BioPharma, LLC, Lowell, Massachusetts 01852, United States*

Mauricio Gil-Silva − *Department of Neuroscience and Center for Advanced Pain Studies, University of Texas at Dallas, Richardson, Texas 75080, United States*

Alejandro Morales − *Department of Neuroscience and Center for Advanced Pain Studies, University of Texas at Dallas, Richardson, Texas 75080, United States*

Avaneesh Rade − *Department of Neuroscience and Center for Advanced Pain Studies, University of Texas at Dallas, Richardson, Texas 75080, United States*

Kevin Joseph Tidgewell − *Graduate School of Pharmaceutical Sciences, Duquesne University, Pittsburgh, Pennsylvania 15282, United States;* orcid.org/0000-0002-0501-2604

Complete contact information is available at: https://pubs.acs.org/10.1021/acsomega.1c05727

Author Contributions

⊥A.T., V.H., and J.L. contributed equally to this study.

Notes

The authors declare the following competing financial interest(s): Three authors are from Young Biopharma, LLC who produced these analogs that were tested. Author affiliation is described.

■ ACKNOWLEDGMENTS

Research reported in this publication was supported by the National Institute on Drug Abuse of the National Institutes of Health under Award Number R43DA050405, the National Institute of Diabetes and Digestive and Kidney Diseases (R01DK115478), and the National Center for Complementary and Integrative Health (R15AT008060). The content is solely the responsibility of the authors and does not necessarily represent the official views of the National Institutes of Health.

■ REFERENCES

(1) Rogers, A. H.; Manning, K.; Garey, L.; Smit, T.; Zvolensky, M. J. Sex differences in the relationship between anxiety sensitivity and opioid misuse among adults with chronic pain. *Addict. Behav.* **2020**, *102*, No. 106156.

(2) Kerckhove, N.; Boudieu, L.; Ourties, G.; Bourdier, J.; Daulhac, L.; Eschalier, A.; Mallet, C. Ethosuximide improves chronic pain-induced anxiety- and depression-like behaviors. *Eur. Neuropsychopharmacol.* **2019**, *29*, 1419−1432.

(3) Paulus, D. J.; Rogers, A. H.; Bakhshaie, J.; Vowles, K. E.; Zvolensky, M. J. Pain severity and prescription opioid misuse among

individuals with chronic pain: The moderating role of alcohol use severity. *Drug Alcohol Depend.* **2019**, *204*, No. 107456.
(4) Nelson, E. K. Capsaicin, The Pungent Principle of Capsicum, and the Detection of Capsicum. *J. Am. Chem. Soc.* **1919**, *41*, 1115−1121.
(5) Frias, B.; Merighi, A. Capsaicin, Nociception and Pain. *Molecules* **2016**, *21*, No. 797.
(6) Caterina, M. J.; Schumacher, M. A.; Tominaga, M.; Rosen, T. A.; Levine, J. D.; Julius, D. The capsaicin receptor: a heat-activated ion channel in the pain pathway. *Nature* **1997**, *389*, 816−824.
(7) Molnar, J. Pharmacologic effects of capsaicin, the sharp tasting principle in paprika. *Arzneimittelforschung* **1965**, *15*, 718−727.
(8) Fattori, V.; Hohmann, M. S. N.; Rossaneis, A. C.; Pinho-Ribeiro, F. A.; Verri, W. A. Capsaicin: Current Understanding of Its Mechanisms and Therapy of Pain and Other Pre-Clinical and Clinical Uses. *Molecules* **2016**, *21*, No. 844.
(9) Ma, X.-L.; Zhang, F.-X.; Dong, F.; Bao, L.; Zhang, X. Experimental evidence for alleviating nociceptive hypersensitivity by single application of capsaicin. *Mol. Pain* **2015**, *11*, No. s12990-015.
(10) Peppin, J. F.; Pappagallo, M. Capsaicinoids in the treatment of neuropathic pain: a review. *Ther. Adv. Neurol. Disord.* **2014**, *7*, 22−32.
(11) Alawi, K.; Keeble, J. The paradoxical role of the transient receptor potential vanilloid 1 receptor in inflammation. *Pharmacol. Ther.* **2010**, *125*, 181−195.
(12) Vyklický, L.; Novakova-Tousova, K.; Benedikt, J.; Samad, A.; Touska, F.; Vlachova, V. Calcium-dependent desensitization of vanilloid receptor TRPV1: a mechanism possibly involved in analgesia induced by topical application of capsaicin. *Physiol. Res.* **2008**, *57*, S59−68.
(13) Anand, P.; Bley, K. Topical capsaicin for pain management: therapeutic potential and mechanisms of action of the new high-concentration capsaicin 8% patch. *Br. J. Anaesth.* **2011**, *107*, 490−502.
(14) Han, P.; McDonald, H. A.; Bianchi, B. R.; Kouhen, R. E.; Vos, M. H.; Jarvis, M. F.; Faltynek, C. R.; Moreland, R. B. Capsaicin causes protein synthesis inhibition and microtubule disassembly through TRPV1 activities both on the plasma membrane and intracellular membranes. *Biochem. Pharmacol.* **2007**, *73*, 1635−1645.
(15) Athanasiou, A.; Smith, P. A.; Vakilpour, S.; Kumaran, N. M.; Turner, A. E.; Bagiokou, D.; Layfield, R.; Ray, D. E.; Westwell, A. D.; Alexander, S. P.; Kendall, D. A.; Lobo, D. N.; Watson, S. A.; Lophatanon, A.; Muir, K. A.; Guo, D. A.; Bates, T. E. Vanilloid receptor agonists and antagonists are mitochondrial inhibitors: how vanilloids cause non-vanilloid receptor mediated cell death. *Biochem. Biophys. Res. Commun.* **2007**, *354*, 50−55.
(16) Kennedy, W. R.; Vanhove, G. F.; Lu, S. P.; Tobias, J.; Bley, K. R.; Walk, D.; Wendelschafer-Crabb, G.; Simone, D. A.; Selim, M. M. A randomized, controlled, open-label study of the long-term effects of NGX-4010, a high-concentration capsaicin patch, on epidermal nerve fiber density and sensory function in healthy volunteers. *J. Pain* **2010**, *11*, 579−587.
(17) Malmberg, A. B.; Mizisin, A. P.; Calcutt, N. A.; von Stein, T.; Robbins, W. R.; Bley, K. R. Reduced heat sensitivity and epidermal nerve fiber immunostaining following single applications of a high-concentration capsaicin patch. *Pain* **2004**, *111*, 360−367.
(18) Robbins, W. R.; Staats, P. S.; Levine, J.; Fields, H. L.; Allen, R. W.; Campbell, J. N.; Pappagallo, M. Treatment of Intractable Pain with Topical Large-Dose Capsaicin: Preliminary Report. *Anesth. Analg.* **1998**, *86*, 579−583.
(19) Costanzo, M. T.; Yost, R. A.; Davenport, P. W. Standardized method for solubility and storage of capsaicin-based solutions for cough induction. *Cough* **2014**, *10*, No. 6.
(20) Glinsukon, T.; Stitmunnaithum, V.; Toskulkao, C.; Buranawuti, T.; Tangkrisanavinont, V. Acute toxicity of capsaicin in several animal species. *Toxicon* **1980**, *18*, 215−220.
(21) Chung, M. K.; Campbell, J. N. Use of Capsaicin to Treat Pain: Mechanistic and Therapeutic Considerations. *Pharmaceuticals* **2016**, *9*, No. 66.
(22) Alsalem, M.; Millns, P.; Altarifi, A.; El-Salem, K.; Chapman, V.; Kendall, D. A. Anti-nociceptive and desensitizing effects of olvanil on capsaicin-induced thermal hyperalgesia in the rat. *BMC Pharmacol. Toxicol.* **2016**, *17*, No. 31.
(23) Ursu, D.; Knopp, K.; Beattie, R. E.; Liu, B.; Sher, E. Pungency of TRPV1 agonists is directly correlated with kinetics of receptor activation and lipophilicity. *Eur. J. Pharmacol.* **2010**, *641*, 114−122.
(24) Nadezhdin, K. D.; Neuberger, A.; Nikolaev, Y. A.; Murphy, L. A.; Gracheva, E. O.; Bagriantsev, S. N.; Sobolevsky, A. I. Extracellular cap domain is an essential component of the TRPV1 gating mechanism. *Nat. Commun.* **2021**, *12*, No. 2154.
(25) Elokely, K.; Velisetty, P.; Delemotte, L.; Palovcak, E.; Klein, M. L.; Rohacs, T.; Carnevale, V. Understanding TRPV1 activation by ligands: Insights from the binding modes of capsaicin and resiniferatoxin. *Proc. Natl. Acad. Sci. U.S.A.* **2016**, *113*, E137−E145.
(26) Iida, T.; Moriyama, T.; Kobata, K.; Morita, A.; Murayama, N.; Hashizume, S.; Fushiki, T.; Yazawa, S.; Watanabe, T.; Tominaga, M. TRPV1 activation and induction of nociceptive response by a non-pungent capsaicin-like compound, capsiate. *Neuropharmacology* **2003**, *44*, 958−967.
(27) Walpole, C. S.; Wrigglesworth, R.; Bevan, S.; Campbell, E. A.; Dray, A.; James, I. F.; Perkins, M. N.; Reid, D. J.; Winter, J. Analogues of capsaicin with agonist activity as novel analgesic agents; structure-activity studies. 1. The aromatic "A-region". *J. Med. Chem.* **1993**, *36*, 2362−2372.
(28) Chen, J.; Lake, M. R.; Sabet, R. S.; Niforatos, W.; Pratt, S. D.; Cassar, S. C.; Xu, J.; Gopalakrishnan, S.; Pereda-Lopez, A.; Gopalakrishnan, M.; Holzman, T. F.; Moreland, R. B.; Walter, K. A.; Faltynek, C. R.; Warrior, U.; Scott, V. E. Utility of large-scale transiently transfected cells for cell-based high-throughput screens to identify transient receptor potential channel A1 (TRPA1) antagonists. *J. Biomol. Screening* **2007**, *12*, 61−69.
(29) Walpole, C. S.; Wrigglesworth, R.; Bevan, S.; Campbell, E. A.; Dray, A.; James, I. F.; Masdin, K. J.; Perkins, M. N.; Winter, J. Analogues of capsaicin with agonist activity as novel analgesic agents; structure-activity studies. 2. The amide bond "B-region". *J. Med. Chem.* **1993**, *36*, 2373−2380.
(30) Walpole, C. S.; Wrigglesworth, R.; Bevan, S.; Campbell, E. A.; Dray, A.; James, I. F.; Masdin, K. J.; Perkins, M. N.; Winter, J. Analogues of capsaicin with agonist activity as novel analgesic agents; structure-activity studies. 3. The hydrophobic side-chain "C-region". *J. Med. Chem.* **1993**, *36*, 2381−2389.
(31) Feng, C.; Loh, T. P. Rhodium(III)-catalyzed cross-coupling of alkenylboronic acids and N-pivaloyloxylamides. *Org. Lett.* **2014**, *16*, 3444−3447.
(32) Mandadi, S.; Numazaki, M.; Tominaga, M.; Bhat, M. B.; Armati, P. J.; Roufogalis, B. D. Activation of protein kinase C reverses capsaicin-induced calcium-dependent desensitization of TRPV1 ion channels. *Cell Calcium* **2004**, *35*, 471−478.
(33) Koplas, P. A.; Rosenberg, R. L.; Oxford, G. S. The role of calcium in the desensitization of capsaicin responses in rat dorsal root ganglion neurons. *J. Neurosci.* **1997**, *17*, 3525−3537.
(34) Gilbert, P. E.; Martin, W. R. The effects of morphine and nalorphine-like drugs in the nondependent, morphine-dependent and cyclazocine-dependent chronic spinal dog. *J. Pharmacol. Exp. Ther.* **1976**, *198*, 66−82.
(35) Tjølsen, A.; Berge, O. G.; Hunskaar, S.; Rosland, J. H.; Hole, K. The formalin test: an evaluation of the method. *Pain* **1992**, *51*, 5−17.
(36) Perkins, M. N.; Campbell, E. A. Capsazepine reversal of the antinociceptive action of capsaicin in vivo. *Br. J. Pharmacol.* **1992**, *107*, 329−333.
(37) Shen, Y.; Boivin, R.; Yoneda, N.; Du, H.; Schiller, S.; Matsushima, T.; Goto, M.; Shirota, H.; Gusovsky, F.; Lemelin, C.; Jiang, Y.; Zhang, Z.; Pelletier, R.; Ikemori-Kawada, M.; Kawakami, Y.; Inoue, A.; Schnaderbeck, M.; Wang, Y. Discovery of anti-inflammatory clinical candidate E6201, inspired from resorcylic lactone LL-Z1640-2, III. *Bioorg. Med. Chem. Lett.* **2010**, *20*, 3155−3157.
(38) Shen, Y.; Du, H.; Kotake, M.; Matsushima, T.; Goto, M.; Shirota, H.; Gusovsky, F.; Li, X.; Jiang, Y.; Schiller, S.; Spyvee, M.; Davis, H.; Zhang, Z.; Pelletier, R.; Ikemori-Kawada, M.; Kawakami,

https://doi.org/10.1021/acsomega.1c05727
ACS Omega 2022, 7, 2929−2946

Y.; Inoue, A.; Wang, Y. Discovery of an in vitro and in vivo potent resorcylic lactone analog of LL-Z1640-2 as anti-inflammatory lead, II. *Bioorg. Med. Chem. Lett.* **2010**, *20*, 3047−3049.
(39) Assadieskandar, A.; Yu, C.; Maisonneuve, P.; Liu, X.; Chen, Y. C.; Prakash, G. K. S.; Kurinov, I.; Sicheri, F.; Zhang, C. Effects of rigidity on the selectivity of protein kinase inhibitors. *Eur. J. Med. Chem.* **2018**, *146*, 519−528.
(40) Govindarajan, V. S.; Sathyanarayana, M. N. Capsicum–production, technology, chemistry, and quality. Part V. Impact on physiology, pharmacology, nutrition, and metabolism; structure, pungency, pain, and desensitization sequences. *Crit. Rev. Food Sci. Nutr.* **1991**, *29*, 435−474.
(41) Smutzer, G.; Devassy, R. K. Integrating TRPV1 Receptor Function with Capsaicin Psychophysics. *Adv. Pharmacol. Sci.* **2016**, *2016*, No. 1512457.
(42) McNamara, C. R.; Mandel-Brehm, J.; Bautista, D. M.; Siemens, J.; Deranian, K. L.; Zhao, M.; Hayward, N. J.; Chong, J. A.; Julius, D.; Moran, M. M.; Fanger, C. M. TRPA1 mediates formalin-induced pain. *Proc. Natl. Acad. Sci. U.S.A.* **2007**, *104*, 13525−13530.
(43) O'Neill, J.; Brock, C.; Olesen, A. E.; Andresen, T.; Nilsson, M.; Dickenson, A. H. Unravelling the mystery of capsaicin: a tool to understand and treat pain. *Pharmacol. Rev.* **2012**, *64*, 939−971.
(44) Nicolson, T. J.; Mellor, H. R.; Roberts, R. R. Gender differences in drug toxicity. *Trends. Pharmacol. Sci.* **2010**, *31*, 108−114.
(45) Brederson, J. D.; Kym, P. R.; Szallasi, A. Targeting TRP channels for pain relief. *Eur. J. Pharmacol.* **2013**, *716*, 61−76.
(46) Vos, M. H.; Neelands, T. R.; McDonald, H. A.; Choi, W.; Kroeger, P. E.; Puttfarcken, P. S.; Faltynek, C. R.; Moreland, R. B.; Han, P. TRPV1b overexpression negatively regulates TRPV1 responsiveness to capsaicin, heat and low pH in HEK293 cells. *J. Neurochem.* **2006**, *99*, 1088−1102.
(47) Deering-Rice, C. E.; Stockmann, C.; Romero, E. G.; Lu, Z.; Shapiro, D.; Stone, B. L.; Fassl, B.; Nkoy, F.; Uchida, D. A.; Ward, R. M.; Veranth, J. M.; Reilly, C. A. Characterization of Transient Receptor Potential Vanilloid-1 (TRPV1) Variant Activation by Coal Fly Ash Particles and Associations with Altered Transient Receptor Potential Ankyrin-1 (TRPA1) Expression and Asthma. *J. Biol. Chem.* **2016**, *291*, 24866−24879.
(48) Madisen, L.; Garner, A. R.; Shimaoka, D.; Chuong, A. S.; Klapoetke, N. C.; Li, L.; van der Bourg, A.; Niino, Y.; Egolf, L.; Monetti, C.; Gu, H.; Mills, M.; Cheng, A.; Tasic, B.; Nguyen, T. N.; Sunkin, S. M.; Benucci, A.; Nagy, A.; Miyawaki, A.; Helmchen, F.; Empson, R. M.; Knopfel, T.; Boyden, E. S.; Reid, R. C.; Carandini, M.; Zeng, H. Transgenic mice for intersectional targeting of neural sensors and effectors with high specificity and performance. *Neuron* **2015**, *85*, 942−958.
(49) Tronche, F.; Kellendonk, C.; Kretz, O.; Gass, P.; Anlag, K.; Orban, P. C.; Bock, R.; Klein, R.; Schutz, G. Disruption of the glucocorticoid receptor gene in the nervous system results in reduced anxiety. *Nat. Genet.* **1999**, *23*, 99−103.
(50) Giusti, S. A.; Vercelli, C. A.; Vogl, A. M.; Kolarz, A. W.; Pino, N. S.; Deussing, J. M.; Refojo, D. Behavioral phenotyping of Nestin-Cre mice: implications for genetic mouse models of psychiatric disorders. *J. Psychiatr. Res.* **2014**, *55*, 87−95.
(51) Gmyrek, D. P. Wilbur Lincoln Scoville: the prince of peppers. *Pharm. Hist.* **2013**, *55*, 136−156.
(52) Szolcsanyi, J.; Jancso-Gabor, A. Sensory effects of capsaicin congeners. Part II: Importance of chemical structure and pungency in desensitizing activity of capsaicin-type compounds. *Arzneimittelforschung* **1976**, *26*, 33−37.
(53) Szolcsanyi, J.; Jancso-Gabor, A. Sensory effects of capsaicin congeners I. Relationship between chemical structure and pain-producing potency of pungent agents. *Arzneimittelforschung* **1975**, *25*, 1877−1881.
(54) Karai, L.; Brown, D. C.; Mannes, A. J.; Connelly, S. T.; Brown, J.; Gandal, M.; Wellisch, O. M.; Neubert, J. K.; Olah, Z.; Iadarola, M. J. Deletion of vanilloid receptor 1-expressing primary afferent neurons for pain control. *J. Clin. Invest.* **2004**, *113*, 1344−1352.
(55) He, G. J.; Ye, X. L.; Mou, X.; Chen, Z.; Li, X. G. Synthesis and antinociceptive activity of capsinoid derivatives. *Eur. J. Med. Chem.* **2009**, *44*, 3345−3349.

https://doi.org/10.1021/acsomega.1c05727
ACS Omega 2022, 7, 2929−2946